

SYNTHESIS AND POLYMERIZATIONS OF NOVEL BISPHOSPHONATE-  
CONTAINING METHACRYLATES

by

Özlem Büyükgümüş

B.S., Chemistry, Muğla University, 2009

Submitted to the Institute for Graduate Studies in  
Science and Engineering in partial fulfillment of  
the requirements for the degree of  
Master of Science

Graduate Program in Chemistry

Boğaziçi University

2012

*To my family*

## ACKNOWLEDGEMENTS

I am heartily thankful to my supervisor Prof. Duygu Avcı Semiz whose guidance and support from the initial to the final level helped me to complete this research project.

I would like to thank to my committee members Assoc. Prof. Havva Yağcı Acar and Assoc. Prof. Ersin Acar for their careful and constructive review of the final manuscript.

I am grateful to my lab-mates Ayşe Altın, Burçin Akgün, Özlem Karahan, Zeynep Saraylı Bilgici and Sesil Agopcan who encouraged and supported me during my studies.

I also thank to Assist. Prof. Bart Noordover and my lab-mates especially Juliën Van Velthoven and my officemates for their invaluable suggestions and supports throughout my study in Eindhoven University of Technology and I would also like to thank to all members of Boğaziçi University Chemistry Department, my instructors, my friends and especially the secretary of the department Hülya Metiner for her help and friendship.

Finally, yet importantly, I would like to express my heartfelt thanks to my beloved parents Aysu Büyükgümüş and Fevzi Büyükgümüş and also my unique sister Pelin Büyükgümüş for their endless support, love and confidence in me during my life.

This work was supported by grants from the Scientific and Technological Council of Turkey (TUBITAK) [109S382] and Boğaziçi University Research Fund [6330].

## ABSTRACT

### SYNTHESIS AND POLYMERIZATIONS OF NOVEL BISPHOSPHONATE-CONTAINING METHACRYLATES

In this study, two novel bisphosphonate-containing methacrylates (1 and 2) were synthesized from reaction of ethyl and *tert*-butyl  $\alpha$ -bromomethacrylates with 3,3-bis(diethoxyphosphoryl)propanoic acid. Their photopolymerizations using 2,2'-dimethoxy-2-phenyl acetophenone (DMPA) as photoinitiator at 40 °C gave polymers in 44 and 64% yield. Thermal bulk polymerizations of 1 and 2 using 2,2'-azobis(isobutyronitrile) (AIBN) gave new water soluble bisphosphonate-containing polymers at 23 and 25 % yield with  $M_n$  values of 83000 and 59500 g/mol for poly-1 and poly-2 respectively. Glass transition temperatures were observed for poly-1 and poly-2 at 75 and 85 °C. Thermal bulk and solution copolymerizations of 1 and 2 with poly(ethylene glycol) methyl ether methacrylate (PEGMA) ( $M_n= 950$ ) in three different feed ratios (90:10, 70:30 and 50:50 mol% PEGMA:1 and PEGMA:2) were investigated using AIBN at 65 °C. Water soluble copolymers were obtained only at 70:30 and 50:50 mol % feed ratios in methanol. The lower molecular weight of the copolymers (10000-33000) compared to poly-PEGMA (230000) can be explained by the chain transfer ability of the synthesized monomers. The copolymer compositions determined from the integrated  $^1\text{H}$  NMR spectra of the copolymers indicated incorporation of the synthesized monomers into polymers. The attempts to hydrolyze bisphosphonate groups of monomers 1 and 2 with trimethylsilyl bromide (TMSBr) were not successful. However, one of the copolymers with 50:50 mol% PEGMA: 2 in feed ratio was hydrolyzed using the same reagent. The pH value of the aqueous solution of the hydrolyzed copolymer (5 wt %) was found to be 1.89. The interaction of this copolymer with hydroxyapatite (HAP), a model compound for bone, was investigated using FTIR spectroscopy.

## ÖZET

### BİSFOSFONAT İÇEREN YENİ METAKRİLATLARIN SENTEZ VE POLİMERİZASYONLARI

Bu çalışmada, iki yeni bisfosfonat içeren metakrilat etil ve tert-butil  $\alpha$ -bromometakrilatın 3,3- bis(dietoksifosforil)propanoik asitle olan reaksiyonundan sentezlenmişlerdir. Bisfosfonat içeren metakrilatların fotopolimerizasyonu 2,2'-dimetoksi-2-fenil asetofenon (DMPA) kullanılarak 40 °C' de gerçekleştirildiğinde yüzde 44 ve 64 verimle polimerler vermiştir. Monomer 1 ve 2' nin azobisisobütironitril (AIBN) ile termal kütle ve çözelti polimerizasyonlarından yeni suda çözünebilir bisfosfonat içeren polimerler yüzde 23 ve 25 verimle elde edilmiştir. Polimer 1 ve 2'nin  $M_n$  değerleri 83000 ve 59500 olarak bulunmuştur. Polimer 1 ve 2 için camı geçiş sıcaklıkları 75 ve 85°C olarak gözlenmiştir. Monomer 1 ve 2'nin poli(etilenglikol) metiletermetakrilat (PEGMA) ( $M_n=950$ ) ile üç farklı başlangıç oranındaki (90:10, 70:30 and 50:50 mol% PEGMA:1 and PEGMA:2) kopolimerizasyonları AIBN ile 65 °C'de araştırılmıştır. Suda çözünebilir kopolimerler metanol kullanılarak yapılan kopolimerleşmelerde ve sadece 70:30 ve 50:50 % mol başlangıç oranlarında elde edilmiştir. Poli-PEGMA (230000) ile karşılaştırıldığında sentezlenen kopolimerlerin moleküler ağırlıklarının düşük olması (10000-33000), sentezlenen monomerlerin zincir transfer reaksiyonları yapabilmesi ile açıklanabilir. Kopolimerlerinin integralli  $^1H$  NMR spektrumlarından elde edilen kopolimer kompozisyonları monomerlerin polimerlere katıldığını göstermiştir. Monomer 1 ve 2' nin bisfosfonat gruplarının trimetilsililbromür (TMSBr) ile hidroliz edilmesine yönelik çalışmalar başarılı olmamıştır. Buna karşın, kopolimerlerden 50:50 % mol PEGMA:2 başlangıç oranında olan aynı madde kullanılarak hidroliz edilmiştir. Hidroliz olmuş kopolimerin sulu çözeltisinin (5 % ağı) pH değeri 1.89 olarak bulunmuştur. Bu kopolimerin, kemik için model bir bileşik olan hidroksiapatit ile olan etkileşimi FTIR spektroskopisi kullanılarak incelenmiştir.

## TABLE OF CONTENTS

ABSTRACT.....	v
ÖZET .....	vi
LIST OF FIGURES .....	ix
LIST OF TABLES .....	xii
1. INTRODUCTION .....	1
1.1. Bisphosphonates .....	1
1.2. Applications of Bisphosphonates .....	3
1.2.1. Therapeutic Uses of Bisphosphonates .....	3
1.2.2. The use of Bisphosphonates in Drug and Protein Delivery Systems .....	6
1.2.3. Bisphosphonate-containing Polymers in Drug Delivery .....	8
1.2.4. Bisphosphonate-containing Polymers in Tissue Engineering .....	10
1.2.5. Utility of Bisphosphonates in Self-Etching Adhesives for Dental Applications.....	11
2. OBJECTIVES .....	14
3. EXPERIMENTAL.....	15
3.1. Materials and Apparatus .....	15
3.1.1. Materials .....	15
3.1.2. Apparatus.....	15
3.2. Synthesis of Starting Materials .....	16
3.2.1. Synthesis of <i>tert</i> -Butyl- $\alpha$ -Hydroxymethacrylate (TBHMA) .....	16
3.2.2. Synthesis of <i>tert</i> -Butyl- $\alpha$ -Bromomethacrylate (TBBr) .....	16
3.2.3. Synthesis of Ethyl- $\alpha$ -Hydroxymethacrylate (EHMA).....	17
3.2.4. Synthesis of Ethyl- $\alpha$ -Bromomethacrylate (EBBr).....	18
3.2.5. Synthesis of <i>tert</i> -butyl 3,3-bis(diethoxyphosphoryl) propanoate .....	18
3.2.6. Synthesis of 3,3-bis(diethoxyphosphoryl)propanoic acid .....	19
3.3. Synthesis of Bisphosphonated Methacrylates .....	19
3.3.1. Ethyl 2-((3,3-bis(diethoxyphosphoryl)propanoylox) methyl)acrylate .....	19
3.3.2. <i>Tert</i> -butyl 2-((3,3 bis(diethoxyphosphoryl)propanoylox)methyl)acrylate .....	20
3.4. Photopolymerizations .....	20
3.5. Free Radical Polymerizations in Bulk and Solution.....	21

3.5.1. Polymerization Procedure .....	21
3.5.1.2. Thermal Polymerizations.....	21
3.6. Hydrolysis of a Copolymer .....	22
4. RESULTS AND DISCUSSION .....	23
4.1. Monomer Synthesis and Characterization.....	23
4.2. Homopolymerizations .....	28
4.3. Copolymerizations.....	31
4.4. Hydrolysis of polymers .....	37
4.5. Acidity and Interactions with HAP .....	37
5. CONCLUSION.....	40
APPENDIX A: SPECTROSCOPY DATA .....	41
REFERENCES .....	57

## LIST OF FIGURES

Figure 1.1.	Structure of pyrophosphate versus general structure of a bisphosphonate. ...	1
Figure 1.2.	The structural differences of bisphosphonate, phosphonophosphinate and bisphosphonate.....	2
Figure 1.3.	Examples of BP compounds.....	2
Figure 1.4.	Examples of bisphosphonate prodrugs. Structure of estradiol conjugated to abisphosphonate via a cleavable ester bond (A) Structure of bisphosphonate prodrug of gatifloxacin (B).....	7
Figure 1.5.	Hydrolysis of camdronate under physiological conditions releases free, active camptothecin. ....	7
Figure 1.6.	Synthesis of aminomethylenediphosphonic acid (A) and biotinyl-aminomethylenediphosphonic acid triethylammonium salt (AMB-Biotin) (B).....	8
Figure 1.7.	TNP-470- HPMA copolymer conjugation targeted with ALN. ....	10
Figure 1.8.	Pamidronate-containing homopolymer (A) and pamidronate-containing copolymer (B).....	11
Figure 1.9.	Self-etching adhesive monomers containing bisphosphonates with dental applications. ....	12
Figure 1.10.	Phosphonic, bisphosphonic and difluoromethylphosphonic acid containing methacrylic monomers (1, 2 and 3) (A) and $\alpha$ - fluorobisphosphonic acid containing acrylic monomer (B).....	13
Figure 4.1.	Synthesis of monomers 1 and 2. ....	23
Figure 4.2.	$^1\text{H}$ NMR spectra of monomer 2 and intermediate compounds. ....	25
Figure 4.3.	$^{13}\text{C}$ NMR spectrum of monomer 2. ....	26

Figure 4.4. FTIR spectra of monomer 1 and 2. ....	27
Figure 4.5. Polymerization of monomer 1 and 2. ....	28
Figure 4.6. <sup>1</sup> H NMR spectra of monomer 1 and poly-1. ....	30
Figure 4.7. Copolymerization of monomers with PEGMA. ....	31
Figure 4.8. <sup>1</sup> H NMR spectra of poly-2 and 2:PEGMA (50:50 mol%) copolymer. ....	33
Figure 4.9. FTIR spectra of poly-2 and 2:PEGMA (50:50 mol%) copolymer. ....	34
Figure 4.10. Rate-time and conversion-time curves in the polymerizations of 1 and 2. ....	35
Figure 4.11. Rate-time and conversion-time curves in the polymerizations of 2 and 2:HEMA (30-70 mol %), 2:HEMA (50-50 mol %) HEMA. ....	36
Figure 4.12. <sup>1</sup> H NMR spectra of 2:PEGMA (50:50 mol%) copolymer (α) and hydrolyzed 2:PEGMA (50:50 mol%) copolymer (β). ....	38
Figure 4.13. FTIR spectra of hydrolyzed copolymer 2:PEGMA (50:50 mol%) with 15 and 30 mg HAP. ....	39
Figure A.1. <sup>1</sup> H NMR spectra of 3,3- bis(diethoxyphosphoryl)propanoate in CDCl <sub>3</sub> . ....	41
Figure A.2. <sup>1</sup> H NMR spectra of 3,3- bis(diethoxyphosphoryl)propanoic acid in CDCl <sub>3</sub> . ....	43
Figure A.3. <sup>1</sup> H NMR spectra of monomer 1 in CDCl <sub>3</sub> . ....	44
Figure A.4. <sup>1</sup> H NMR spectra of monomer 2 in CDCl <sub>3</sub> . ....	45
Figure A.5. FTIR spectrum of monomer 1. ....	46
Figure A.6. FTIR spectrum of monomer 2. ....	47
Figure A.7. <sup>1</sup> H NMR Spectrum of polymer 1 in CDCl <sub>3</sub> . ....	48
Figure A.8. <sup>1</sup> H NMR Spectrum of polymer 2 in MeOD. ....	49

Figure A.9. $^1\text{H}$ NMR Spectrum of copolymer 1: PEGMA (50:50 mol%) in MeOD.....	50
Figure A.10. $^1\text{H}$ NMR Spectrum of copolymer 2: PEGMA (50:50 mol%) in MeOD.....	51
Figure A.11. $^1\text{H}$ NMR spectrum of hydrolysed copolymer 2: PEGMA (50:50 mol%) in MeOD. ....	52
Figure A.12. FTIR spectrum of copolymer 1: PEGMA (50:50 mol%). ....	53
Figure A.13. FTIR spectrum of copolymer 2: PEGMA (50:50 mol%). ....	54
Figure A.14. FTIR spectrum of hydrolysed copolymer 2: PEGMA (50:50 mol%).....	55
Figure A.15. FTIR spectrum of hydrolysed copolymer 2: PEGMA (50:50 mol%) after addition of 30 mg HAP.....	56

## LIST OF TABLES

Table 1.1. Commercially Available Bisphosphonate Drugs. ....	4
Table 4.1. Solubility of Monomers and Polymers.....	24
Table 4.2. Thermal Homo- and Copolymerization of the Bisphosphonate Monomers with PEGMA. ....	29

**LIST OF ACRONYMS/ABBREVIATIONS**

AIBN	2,2'-azobisisobutyronitrile
DMPA	2,2'-dimethoxy-2-phenylacetophenone
DSC	Differential Scanning Calorimetry
EBBR	Ethyl- $\alpha$ -Bromomethyl Acrylate
EBHMA	Ethyl- $\alpha$ -Hydroxymethyl Acrylate
FT-IR	Fourier Transform Infrared Spectroscopy
GPC	Gel Permeation Chromatography
HAP	Hydroxyapatite
HEMA	2-Hydroxyethyl methacrylate
NMR	Nuclear Magnetic Resonance Spectroscopy
$R_p$	Rate of polymerization
TBBR	<i>tert</i> -Butyl- $\alpha$ -Bromomethyl Acrylate
TBHMA	<i>tert</i> -Butyl- $\alpha$ -Hydroxymethyl Acrylate
TEA	Triethylamine
$T_g$	Glass transition temperature

## 1. INTRODUCTION

### 1.1. Bisphosphonates

Bisphosphonates (BPs) are structural analogues of naturally occurring pyrophosphate with increased chemical and enzymatic stability due to the replacement of the oxygen in P-O-P by a carbon, resulting in a P-C-P structure (Figure 1.1) [1].

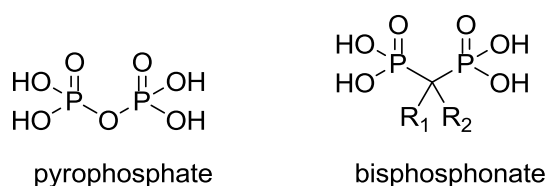


Figure 1.1. Structure of pyrophosphate versus general structure of a bisphosphonate.

Small changes in the structure of the bisphosphonates can give rise to extensive alterations in their physicochemical, biological, therapeutic, and toxicological characteristics.

The ability of bisphosphonates to inhibit bone resorption is due to their high affinity for bone mineral, hydroxyapatite (HAP): The P-C-P motif of bisphosphonates can chelate calcium ions by bidentate coordination with the help of the oxygen atoms of the phosphonate groups. Studies show that the affinity of bisphosphonates to calcium ions will change via modifications of the phosphonate groups (e.g. methylation of one or both phosphonates to produce phosphonophosphinates or bisphosphinates, respectively) or substitution of P-C-P bonds with P-N-P or P-C-C-P bonds (Figure 1.2) [2].

The bone affinity of bisphosphonates can be enhanced further by choice of the side chains  $R_1$  and  $R_2$ . When the  $R_1$  side chain is a hydroxyl (-OH) group (as in pamidronate), bisphosphonates can bind calcium ions more effectively because this allows tridentate coordination to calcium ions. The  $R_2$  side-chain can be used to classify bisphosphonates into those that contain nitrogen in their side chains (pamidronate, neridronate, olpadronate, alendronate, ibandronate, risendronate and zoledronate), and those that do not (etidronate, clodronate, and tiludronate). The amino-containing bisphosphonate derivatives are found to be more active than non-amino containing ones due to antiresorptive potency [3].

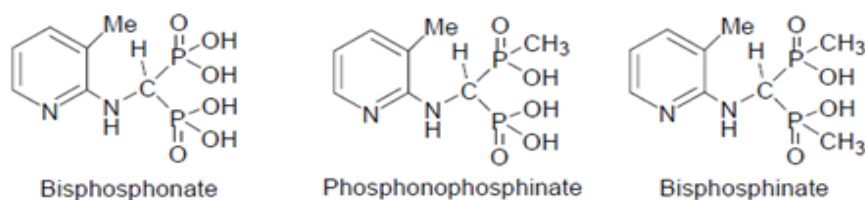


Figure 1.2. The structural differences of bisphosphonate, phosphonophosphinate and bisphosphonate.

These properties of BPs have been utilized to design and synthesize a vast array of bone-targeting compounds. The most commonly used bisphosphonates as antiresorptive and bone-seeking agents are shown in Figure 1.3.

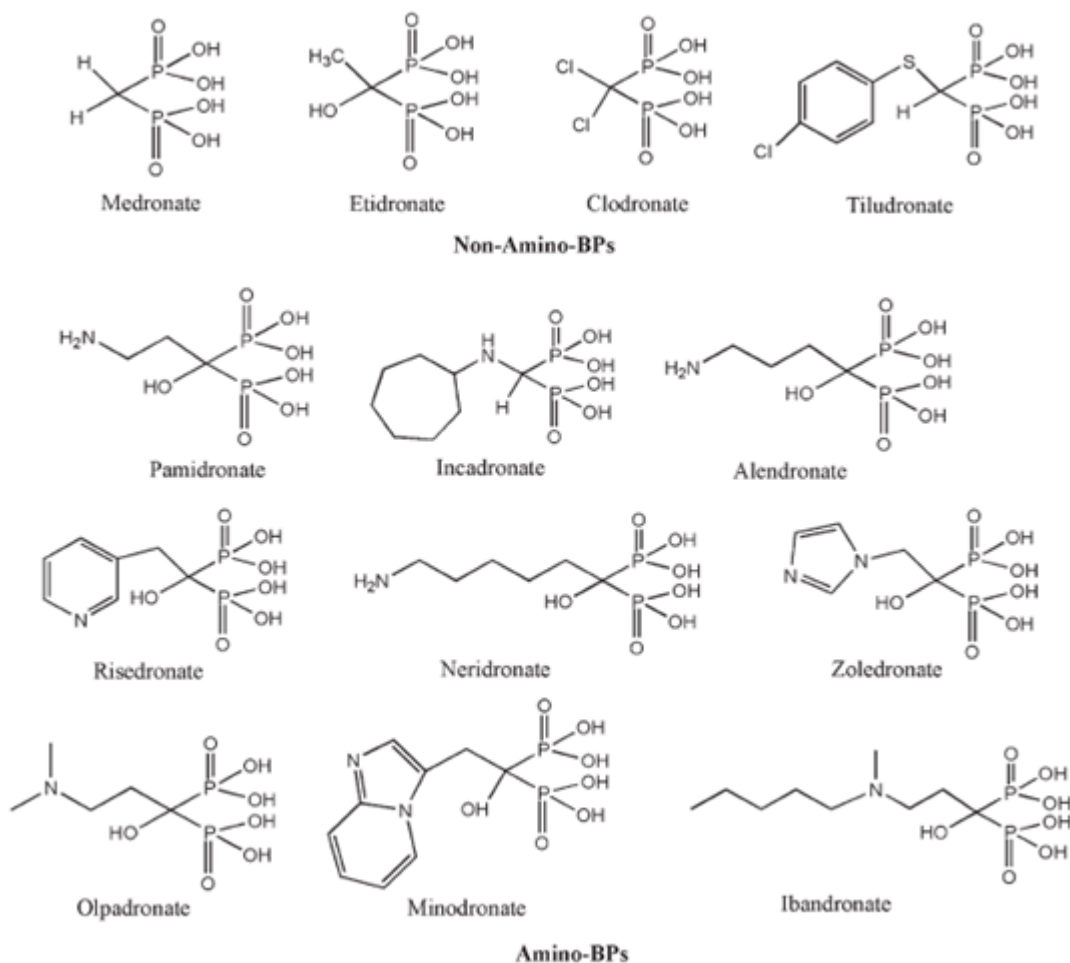


Figure 1.3. Examples of BP compounds.

## 1.2. Applications of Bisphosphonates

### 1.2.1. Therapeutic Uses of Bisphosphonates

Although a range of therapeutic agents is available to treat skeletal disorders [4], their clinical application is hampered by their uptake in non-targeted sites and the consequent undesired side effects [5]. To minimize these, active targeting with controlled delivery is desirable.

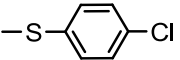
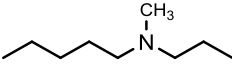
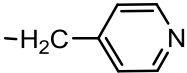
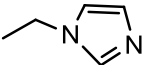
Bisphosphonates (BPs) are known to have high affinity to bone mineral and inhibit bone resorption [6,7], they are widely used in treatment of bone related diseases. They are well-suited to deliver small molecule drugs [8-11], imaging agents [12,13] and peptides or proteins to the bone [14,15]. Table 1.1 shows relative potencies, routes of administration and indications of these bisphosphonate drugs. Bone affinity and antiresorptive abilities appear to depend on separate properties of bisphosphonate structure [16,17].

For example, bisphosphonates are the therapy of choice in Paget's disease. The compound most often used was, and possibly still is, pamidronate. The bisphosphonates decrease bone turnover, often to normal values, they improve the morphology of bone, and ameliorate bone pain. The effect often persists over a long time after discontinuation of the treatment.

A treatment for osteoporosis that is again gaining popularity is bisphosphonate therapy. Various bisphosphonates have been investigated in osteoporosis, the compounds investigated most thoroughly being alendronate and risedronate. The bisphosphonates not only prevent bone loss, but can actually also strengthen bone mineral density. Furthermore, the vertebral and non-vertebral fracture incidence is diminished by about one-half upon bisphosphonate therapy. Bisphosphonates are active in, among others, postmenopausal and elderly women, in men, and in corticosteroid-treated patients.

Finally, bisphosphonates are the drugs of choice to decrease bone resorption in tumor bone disease. The therapy induces a diminution of bone resorption, leading to a decrease in hypercalcemia, a decrease of new osteolytic lesions and a decrease of fractures, and leading to an amelioration of pain and an improvement of the quality of life [2,18].

Table 1.1. Commercially Available Bisphosphonate Drugs.

(Trade Name)	R <sub>1</sub>	R <sub>2</sub>	Relative Potency	Route	Indication(s)
Etidronate (Didrocal, Didronel)	-OH	-CH <sub>3</sub>	1	oral or intravenous	Paget's disease, heterotopic ossification
Clodronate (Bonafos, Ostac)	-Cl	-Cl	10X	oral daily or intravenous	hypercalcaemia of malignancy
Tiludronate (Skelid)	-H		10X	oral daily	Paget's disease
Pamidronate (Aredia)	-OH	-(CH <sub>2</sub> ) <sub>2</sub> NH <sub>2</sub>	100X	intravenous	Paget's disease, hypercalcaemia of malignancy, breast cancer
Alendronate (Fosamax)	-OH	-(CH <sub>2</sub> ) <sub>3</sub> NH <sub>2</sub>	>10-1000X	oral weekly	osteoporosis, Paget's disease
Ibandronate (Boniva, Bondronat)	-OH		>1000-10000X	oral monthly	Paget's disease, osteoporosis, hypercalcaemia of malignancy
Risedronate (Actonel)	-OH		5000-10000X	oral weekly	Paget's disease, osteoporosis
Zoledronic acid (Zometa)	-OH		>10000X	intravenous or infusion	hypercalcaemia of malignancy

### 1.2.2. The Use of Bisphosphonates in Drug and Protein Delivery Systems

In delivery systems, BPs are typically covalently attached to either a drug or protein for site-specific transport to bone. Anticancer, antibacterial, or anti-osteoporosis agents have recently been coupled to BPs to form novel delivery systems [18]. For instance, although hormone replacement therapy is considered an effective treatment for postmenopausal osteoporosis, systemic adverse side effects, including risk of cancer, are possible due to the presence of estrogen receptors in several tissues [19]. Thus, BP prodrugs are investigated in the hope that the BP will deliver the drug to bone and enzymatic and/or chemical mechanisms will subsequently release the active drug, hence alleviate this issue.

Thus, estradiol was conjugated to a BP via a cleavable ester bond and was shown to be much more effective than the parent drug alone, indicating site-specific and sustained therapeutic effects on bone (Figure 1.4a). More recently, bisphosphonate prodrugs of fluoroquinolone conjugates have also been reported for the treatment of bone related diseases such as osteomyelitis, an inflammatory process resulting from an underlying microbial infection and accompanied by bone necrosis. Antibacterial agents to treat this disease face many challenges, including a physiological environment that is difficult for the immune system to access and that highly favors bacterial cells to improve their resistance. Therefore, prodrugs that deliver the antibacterial directly to the bone where the drug would be released would address these therapeutic challenges. 94.7% of the exemplary BP-derived compound shown in Figure 1.4b was bound to bone within 1 hour alone, demonstrating that the prodrug maintained a high affinity for osseous tissues [8,19]. Additionally, the compound not only demonstrated reasonable rates for releasing the parent drug, but also efficiently.

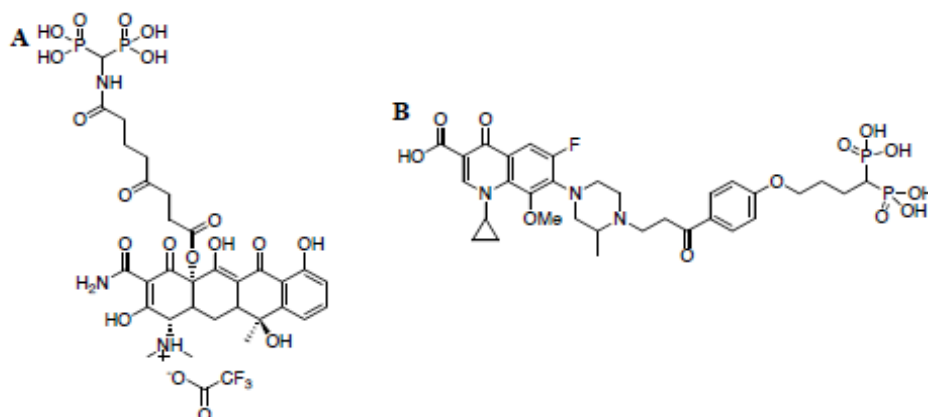


Figure 1.4. Examples of bisphosphonate prodrugs. Structure of estradiol conjugated to a bisphosphonate via a cleavable ester bond (A) Structure of bisphosphonate prodrug of gatifloxacin (B).

Erez *et. al.* attached a bisphosphonate moiety to the known chemotherapeutic drug camptothecin. In clinical trials, camptothecin was not found effective due to its excessively low aqueous solubility and a variety of serious toxic side effects. Camptothecin was esterified with bisphosphonate-butyric acid to form an esterolytic-activated prodrug (Figure 1.5). As a consequence, the prodrug successfully bound to HAP, a model for bone and was hydrolytically activated under physiological conditions. In the Jurksat cell line, it was found 10-fold less toxic than free camptothecin [20].

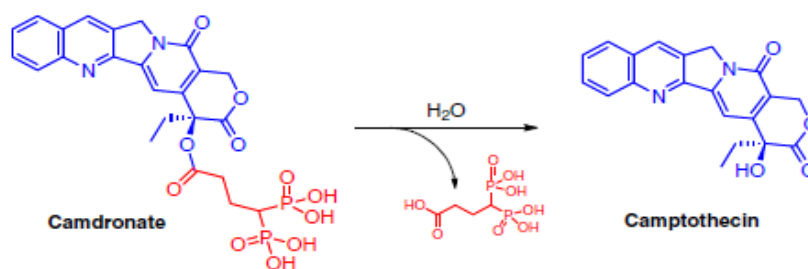


Figure 1.5. Hydrolysis of camdronate under physiological conditions releases free, active camptothecin.

Ehrlich *et al.* synthesized an aminobisphosphonate covalently conjugated with biotin as a model linker for protein attachment to bone (Figure 1.6). Their study indicated that modified aminobisphosphonate conjugates can bind hydroxyapatite and bone at high levels, while the biotin functionality is free to be recognized by the fluorescently labeled anti-biotin antibody [21].

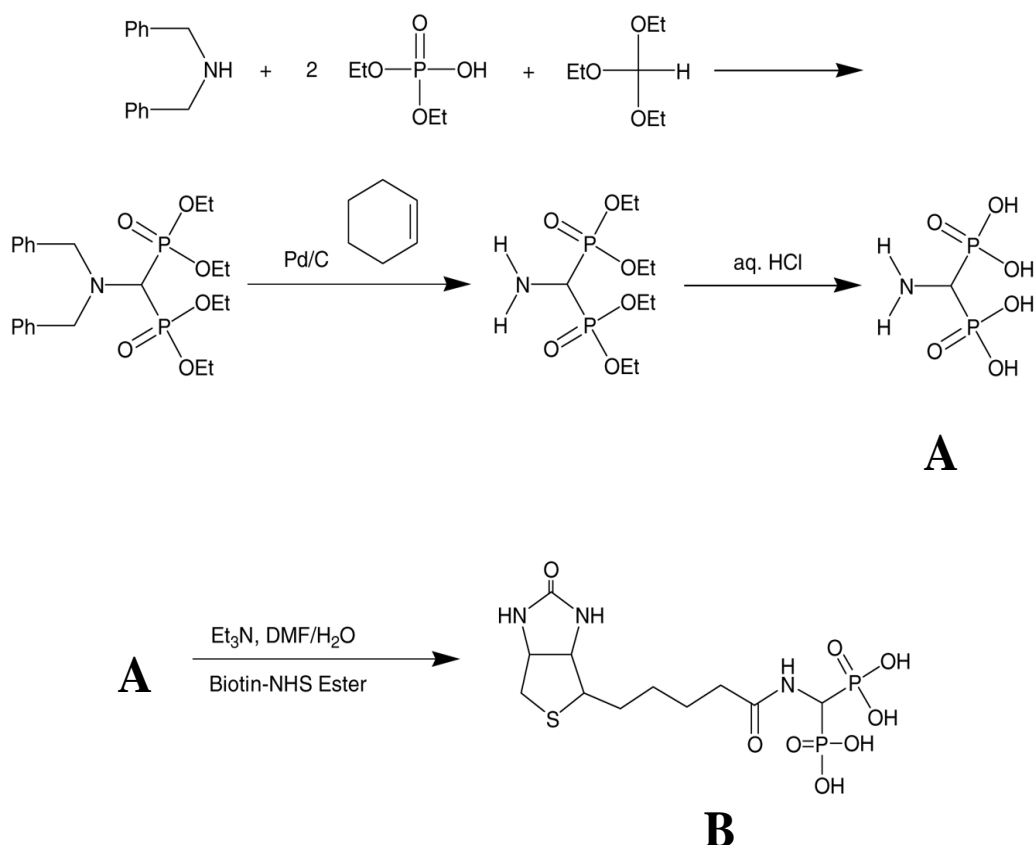


Figure 1.6. Synthesis of aminomethylenediphosphonic acid (A) and biotinyl-aminomethylenediphosphonic acid triethylammonium salt (AMB-Biotin) (B).

### 1.2.3. Bisphosphonate-containing Polymers in Drug Delivery

Polymers carrying high density of bone-targeting groups will obviously have advantages over the corresponding small molecules. These polymer-drug conjugates are expected to both decrease the toxicity of drugs and improve their therapeutic efficiency by increasing half-life of drugs in circulation, solubility and biodistribution of drugs. Incorporation of a targeting moiety, a drug release mechanism, drug selection and physical

characteristics of the polymer carrier are all essential elements in the development of bone-targeting macromolecular therapeutics.

Although bisphosphonates are excellent therapeutic agents, there are only a few reports about incorporation of bisphosphonates into polymers: Bone-targeting drug conjugates based on poly(ethylene glycol) and poly[N-(2-hydroxypropyl)methacrylamide] containing alendronate as bone targeting groups were tested (Figure 1.7)[22-25].

Miller *et al.* used alendronate (ALN) targeted paclitaxel (PTX) containing [N-(2-hydroxypropyl)methacrylamide] (HPMA) copolymers to decrease migration and proliferation of human prostate adenocarcinoma (PC3) cells. They incorporated an enzymatically cleavable linker (GFLG) for both PTX and ALN. *In vitro* data demonstrated that the HPMA copolymer prevented migration and proliferation of the prostate cancerous cell [24].

In a follow up study Miller *et al.* showed the *in vivo* tumor inhibition and safety profiles on Balb/c mice. The PTX, ALN, HPMA copolymer demonstrated no significant toxicity while free PTX significantly reduced white blood cell (WBC) counts. Intratibial injections of mCherrylabeled 4 T1 cells were used to mimic breast cancer metastasis to the bone. Following administration of either PTX, ALN HPMA copolymer or free PTX+ALN in combination, the polymer conjugate inhibited tumor growth by 60%, while free PTX+ALN only inhibited 37% as compared to controls [25].

Segal *et al.* conducted a similar set of experiments using TNP-470 bound to an HPMA copolymer conjugate targeted with ALN (Figure 1.7). TNP-470 is an anticancer agent which showed high efficacy in clinical trials but a great many side effects prevented clinical applications [26].

Segal *et al.* sought to reduce TNP-470 side effects by conjugation and targeting. Both ALN and TNP-470 were attached to HPMA using Cat K sensitive linkers (Gly-Gly-Pro-Nle). *In vivo* studies indicated (Figure 1.7) that not only do ALN and TNP-470 have synergism, but revealed that the HPMA copolymer induced a decrease in osteosarcoma growth by 96% compared to the control, as opposed to 45% with free ALN in combo with TNP-470[27].

Similar to the PTX, ALN, HPMA copolymer, TNP-470, ALN, HPMA copolymer's toxicity is low, as opposed to ALN+TNP-470, which caused in vivo weight loss, neurological dysfunction, and low WBC counts [28]. While ALN facilitates the delivery of a drug to the bones, the conjugation with a polymer provides targeting to tumor tissue within the bones.

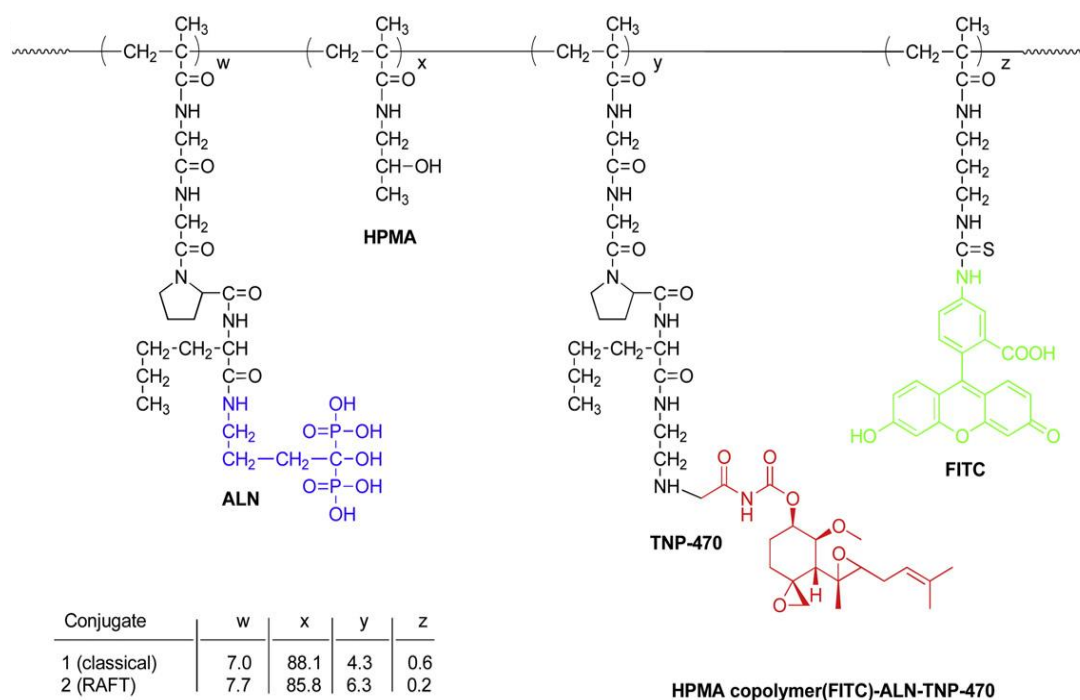


Figure 1.7. TNP-470- HPMA copolymer conjugation targeted with ALN.

#### 1.2.4. Bisphosphonate-containing Polymers in Tissue Engineering

In recent years, biomaterials from ceramics to polymers have been investigated to be better integrated with natural bone and can be used in bone for applications such as total hip replacement, dental implants, and screws for fracture fixation [29-31]. Composites containing continuous calcium phosphate with a dispersed synthetic biodegradable polymer component were prepared.

In addition to composite preparation, many approaches using biomimetic principles to mineralize polymer scaffolds were developed. Natural bone consists of a matrix of

collagen upon which carbonated apatite deposition occurs. Anionic proteins serve as nucleators and inhibitors [32].

Another approach is the functionalization of biomaterials with negatively charged functional groups which provide nucleating sites to induce mineralization of polymer scaffolds [33-35]. The incorporation of anions such as carboxylate or oxyphosphorus (e.g. phosphate, phosphonate) groups into polymeric substrates is inspired from the nature and gives biomaterials with the calcification ability. Phosphorus-containing anionic functional groups are among the most efficient groups for mineralization.

For example, a hydrogel prepared from copolymer of N-acrylamidronate and N-isopropylacrylamide was used as scaffold for mineralization of HAP [36] (Figure 1.8). Bisphosphonate derivatives of cationic polymers such as poly(l-lysine) and poly(ethylenimine) were tested for affinity to HAP [37] and bisphosphonate-modified polyurethanes were prepared to resist calcification around implants [38].

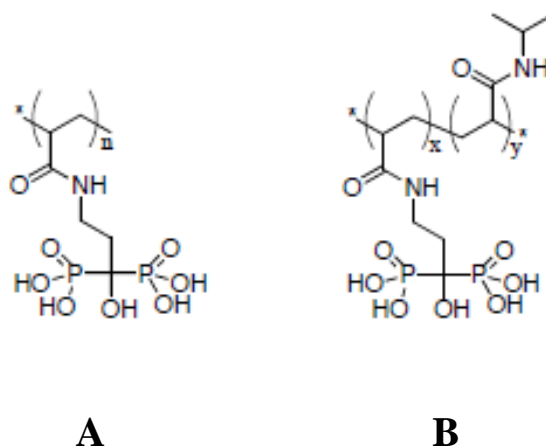


Figure 1.8. Pamidronate-containing homopolymer (A) and pamidronate-containing copolymer (B).

### 1.2.5. Utility of Bisphosphonates in Self-Etching Adhesives for Dental Applications

Although filling materials have been widely used in the past decade, their current formulations, fillers, and enamel and dentin bonding agents urgently need to be improved to increase their clinical performance. Specifically, self-etching enamel-dentin adhesives,

which are based on polymerizable, strongly acidic monomers, are used to modify dental hard tissues (enamel and dentin) and provide strong bonding between a restorative composite and these tissues [39].

More recently bisphosphonate-containing monomers were investigated for self-etching dental adhesive applications [40] which facilitate adhesion of dental restoratives and orthodontic appliances to dental tissue. Additionally, since it is reported that bisphosphonates can inhibit enzymes matrix metalloproteinases (MMPs) which have ability to degrade extracellular matrix, the use of such acidic monomers in dental SEAs should prevent collagen disruption [41].

Some literature examples of self-etching dental adhesive monomers containing bisphosphonates are shown in Figure 1.9.

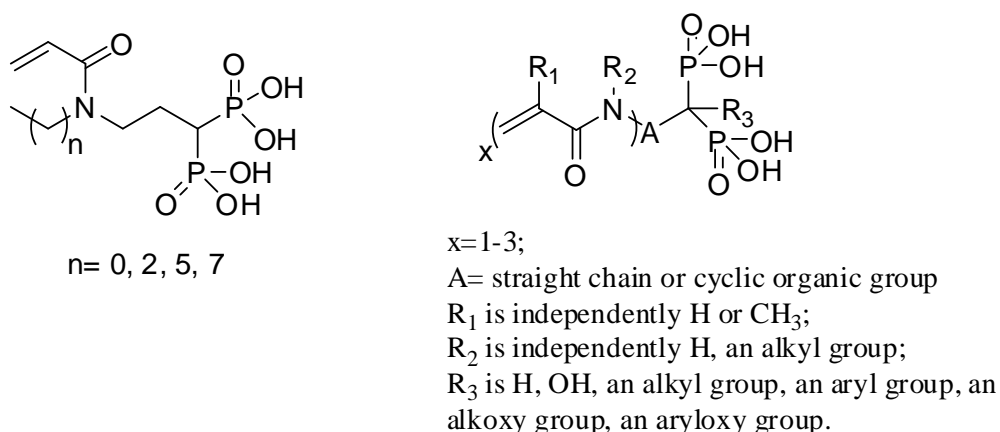


Figure 1.9. Self-etching adhesive monomers containing bisphosphonates with dental applications.

Catel *et al.* synthesized novel self-etching monomers (1, 2 and 3) containing phosphonic acid, bisphosphonic acid and difluoromethylphosphonic acid functionality respectively (Figure 1.10A). They evaluated these monomers in terms of their acidity, HAP interaction, polymerization reactivity and long term stability. It was found that all synthesized monomers were able to efficiently adhere to HAP. Additionally, bisphosphonic acid 2 showed significantly higher reactivity than both phosphonic acid 1 and difluorophosphonic acid 3. These results were mainly attributed to the formation of

hydrogen bonds affecting the system mobility and organization during polymerization. Besides, dentin shear bond strength measurements demonstrated that primers based on the bisphosphonic acid 2 and the difluoromethylphosphonic acid 3 were more efficient than the one based on the corresponding phosphonic acid 1. Therefore, these two monomers appear to be great candidates to enter adhesive formulations. They also suggested that bisphosphonic and difluorophosphonic acids should also improve dentin adhesion durability due to their chelating properties [42].

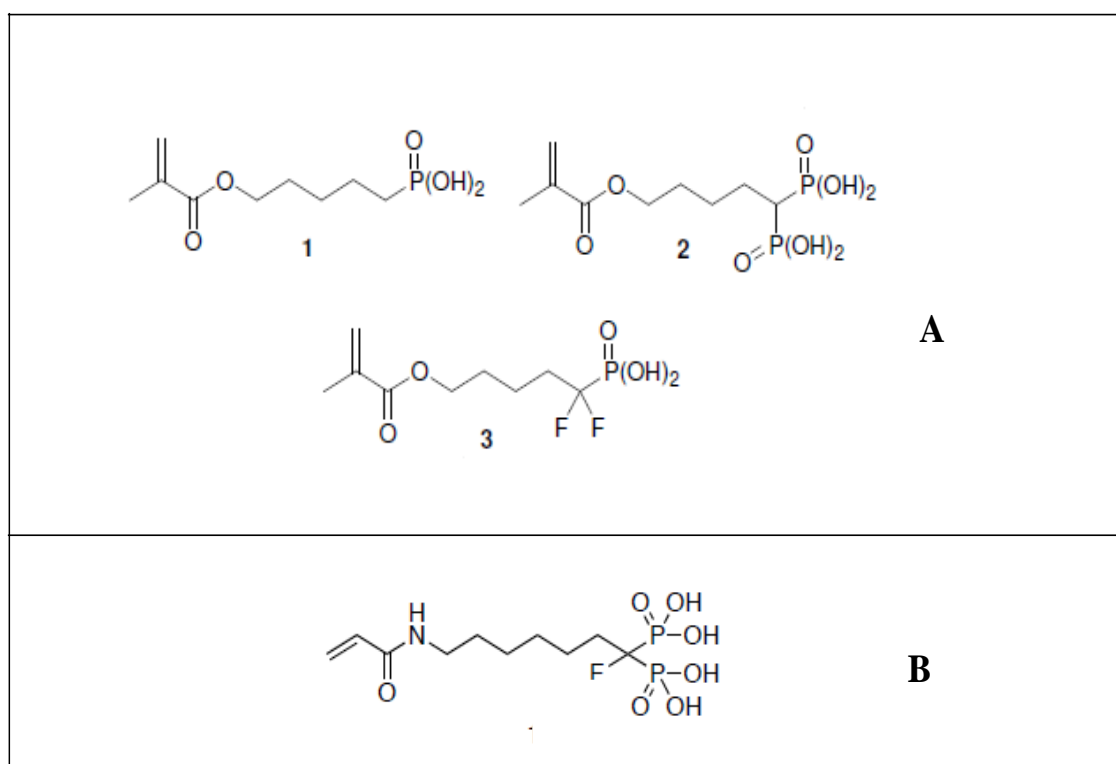


Figure 1.10. Phosphonic, bisphosphonic and difluoromethylphosphonic acid containing methacrylic monomers (1, 2 and 3) (A) and  $\alpha$ -fluorobisphosphonic acid containing acrylic monomer (B).

In a similar study, Bala *et al.* designed and synthesized a novel  $\alpha$ -Fluorobisphosphonic acid tethered by an alkyl chain to acrylamide (Figure 1.10b). The inclusion of a primary  $\alpha$ -amino group at the distal end of the tether attached to the bridging carbon of the BP introduces a chemical functionality that can be easily attached to the acrylic acid monomer via an amide linkage. As a result, the desired self-etching monomer was obtained bearing these key characteristics: increased acidity, improved hydrophobicity and hydrolytic stability [43].

## 2. OBJECTIVES

The aim of this project is to synthesize new bisphosphonate- and bisphosphonicacid-containing monomers and polymers.

These monomers have potential in dental materials and their polymers can be used in bone-targeting drug delivery and tissue engineering applications.

The monomers are derivatives of alkyl  $\alpha$ -hydroxymethacrylates (RHMA) and are expected to have high rate of homo- and copolymerization which is important for dental applications. The homo- and copolymers have both bisphosphonate groups and *tert*-butyl groups which can hydrolyze to bisphosphonic and carboxylic acid functional groups. These groups are important for bone targeting and drug attachment. The polymers can also enhance bone mineralization to be used as scaffolds in tissue engineering applications.

### 3. EXPERIMENTAL

#### 3.1. Materials and Apparatus

##### 3.1.1. Materials

*tert*-Butyl acrylate (Aldrich), paraformaldehyde (Merck), 1,4-diisobicyclo [2.2.2] octane (DABCO) (Aldrich), anhydrous CaCl<sub>2</sub> (Merck), anhydrous Na<sub>2</sub>SO<sub>4</sub> (Merck), CuCl<sub>2</sub>(Merck), hydrochloric acid (Merck), triethylamine (Aldrich), ammonium chloride (Merck), K<sub>2</sub>CO<sub>3</sub> (Merck), PBr<sub>3</sub>(Aldrich), NaCl (Merck), NaHCO<sub>3</sub>(Merck),NaH (Aldrich), tetraethylmethylen bisphosphonate (Aldrich), trimethylsilyl bromide (TMSBr) (Aldrich), trifluoro acetic acid(Aldrich), hydroxyapatite (HAP) (Aldrich),2-hydroxyethyl methacrylate (HEMA, Aldrich), hexane (Merck), diethyl ether (Merck), 2,2'-azobis(isobutyronitrile) (AIBN, Aldrich),poly(ethylene glycol) methyl ether methacrylate (PEGMA) (M<sub>w</sub> =950 g/mol), 2,2'-dimethoxy-2-phenyl acetophenone (DMPA, Aldrich), methanol (Merck), methyl ethyl ketone(Merck)were used as received.

Dimethyl formamide was dried over activated molecular sieves (4 Å<sup>0</sup>) and distilled prior touse.Solvents for chromatography (hexane and ethyl acetate) were received from a chemical company and distilled before used.

##### 3.1.2. Apparatus

The monomer characterization involved <sup>1</sup>H, <sup>13</sup>C and <sup>31</sup>P NMR spectroscopy (Varian Gemini 400 MHz) and Fourier transform infrared (FTIR) spectroscopy (T 380). The photopolymerizations were carried out on a TA Instruments Q100 differential photocalorimeter (DPC). Gel permeation chromatography (GPC) was performed on a Viscotek apparatus equipped with a refractive index detector, using THF solvent and polystyrene standards.

## 3.2. Synthesis of Starting Materials

### 3.2.1. Synthesis of *tert*-Butyl- $\alpha$ -Hydroxymethacrylate (TBHMA)

*tert*-Butyl acrylate (128.12 g, 1 mol), paraformaldehyde (30 g, 1 mol), 1,4-diazobicyclo [2.2.2] octane (DABCO) (14 g, 0.125 mol), dimethylsulfoxide (227 mL) and water (85 mL) were added to a 1000 mL round bottom flask and placed in a oil bath at 70°C. After the reaction mixture was heated at 90 °C for 30 min, it was cooled and aqueous phase was separated. The organic phase was washed with 1 wt per cent HCl (2x100 mL),dried with anhydrous CaCl<sub>2</sub> and filtered. The solution was then distilled under reducedpressure in the presence of a free radical inhibitor, CuCl<sub>2</sub>, and pure TBHMA was collectedas a colorless liquid in 30-40 % yield [44-46].

<sup>1</sup>H NMR (CDCl<sub>3</sub>): 1.5 (s, 9H, CH<sub>3</sub>), 2.7 (s, 1H, O-H), 4.2 (s, 2H, CH<sub>2</sub>-O), 5.7, 6.1 (d, 2H, CH<sub>2</sub>=C) ppm.

<sup>13</sup>C NMR (CDCl<sub>3</sub>):  $\delta$  = 27.9 (CH<sub>3</sub>), 62.4 (CH<sub>2</sub>-O), 81.2 [C-(CH<sub>3</sub>)<sub>3</sub>], 124.4 (CH<sub>2</sub>=C), 140.6 (C=CH<sub>2</sub>), 165.4 (C=O) ppm.

FT-IR: 3420 (OH), 2978-2934 (C-H), 1709 (C=O), 1639 (C=C), 1159-1054 (C-O) cm<sup>-1</sup>.

### 3.2.2. Synthesis of *tert*-Butyl- $\alpha$ -Bromomethacrylate (TBBr)

To a solution of TBHMA (21.24 g, 134.4 mmol) in 130 mL of ether, PBr<sub>3</sub> (6 mL, 63mmol) was added dropwise in an ice bath, under nitrogen. The mixture was stirred at room temperature for 3 hours. Then H<sub>2</sub>O (69 mL) was added dropwise to this solution in an ice bath and the aqueous phase was separated. The aqueous phase was extracted with hexane (3x23 mL). The organic phases were combined, washed with saturated NaCl solution (2x23 mL) and dried with anhydrous CaCl<sub>2</sub>. After the removal of ether by rotary evaporator, distillation was done under reduced pressure to obtain pure product in 81 % yield [44-46].

$^1\text{H}$  NMR ( $\text{CDCl}_3$ ): 1.5 (s, 9H,  $\text{CH}_3$ ), 4.1 (s, 2H,  $\text{CH}_2\text{-Br}$ ), 5.8, 6.2 (d, 2H,  $\text{CH}_2\text{=C}$ ) ppm.

$^{13}\text{C}$ -NMR ( $\text{CDCl}_3$ ): 27.9 ( $\text{CH}_3$ ), 29.7 ( $\text{CH}_2\text{-Br}$ ), 81.5 [ $\text{C-(CH}_3)_3$ ], 127.8 ( $\text{CH}_2\text{=C}$ ), 138.8 ( $\text{C=CH}_2$ ), 164.1 ( $\text{C=O}$ ) ppm.

FTIR: 2978-2934 (C-H), 1718 (C=O), 1621 (C=C), 1226-1158 (C-O), 720 (C-Br)  $\text{cm}^{-1}$

### 3.2.3. Synthesis of Ethyl- $\alpha$ -Hydroxymethacrylate (EHMA)

Ethyl acrylate (66.8 g, 0.66 mol), paraformaldehyde (20 g, 0.66mol) and 1,4-diazobicyclo [2.2.2] octane (DABCO) (9.33 g, 0.08 mol) were added to a mixture of DMSO (151 mL) and  $\text{H}_2\text{O}$  (57 mL). The mixture was heated at 60 °C for 30 minutes under  $\text{N}_2$ . Then it was cooled and extracted with diethyl ether (2x70 mL). The combined organic phases were washed with one wt per cent HCl (3x35 mL), dried with anhydrous  $\text{CaCl}_2$  and filtered. After the removal of ether by rotary evaporator, the solution was distilled under reduced pressure and pure EHMA was collected as a colorless liquid in 40-50 per cent yield [44-46].

$^1\text{H}$ -NMR ( $\text{CDCl}_3$ ): 1.24 (t, 3H,  $\text{CH}_3$ ), 2.94 (s, 1H, O-H), 4.15 [q, 2H,  $\text{CH}_2\text{-C(O)}$ ], 4.24 (s, 2H,  $\text{CH}_2\text{-O}$ ), 5.78, 6.18 (d, 2H,  $\text{CH}_2\text{=C}$ ) ppm

$^{13}\text{C}$ -NMR ( $\text{CDCl}_3$ ): 14.53 ( $\text{CH}_3$ ), 61.16 ( $\text{CH}_2\text{-O}$ ), 62.25 ( $\text{CH}_2\text{-OH}$ ), 125.40 ( $\text{C=CH}_2$ ), 139.76 ( $\text{C=CH}_2$ ), 166.40 ( $\text{C=O}$ ) ppm.

FTIR: 3500-3000 (OH), 2983 (C-H), 1710 (C=O), 1637 (C=C)  $\text{cm}^{-1}$ .

### 3.2.4. Synthesis of Ethyl- $\alpha$ -Bromomethacrylate (EBBr)

2.5 mL of  $\text{PBr}_3$  (26.3 mmol) was added to a solution of EHMA (7.25 g, 55.8 mmol) in 50 mL of ether on ice, under nitrogen. After three hours of mixing at room temperature, 30 mL of  $\text{H}_2\text{O}$  was added in an ice bath and the aqueous phase was separated. Then it was extracted with hexane (3x10 mL). The organic phases were combined, washed with saturated NaCl solution (2x10 mL) and dried with anhydrous  $\text{CaCl}_2$ . After the removal of ether by rotary evaporator, distillation was done under reduced pressure to obtain pure product as a colorless liquid in 74.9 per cent yield [44-46].

$^1\text{H-NMR}$  ( $\text{CDCl}_3$ ): 1.30 (t, 3H,  $\text{CH}_3$ ), 4.16 (s, 2H,  $\text{CH}_2\text{-Br}$ ), 4.25 [q, 2H,  $\text{CH}_2\text{-C(O)}$ ], 5.91, 6.30 (d, 2H,  $\text{CH}_2\text{=C}$ ) ppm.

$^{13}\text{C-NMR}$  ( $\text{CDCl}_3$ ): 14.14 ( $\text{CH}_3$ ), 29.31 ( $\text{CH}_2\text{-Br}$ ), 61.10 ( $\text{CH}_2\text{-O}$ ), 128.48 ( $\text{C=CH}_2$ ), 137.39 ( $\text{C=CH}_2$ ), 164.36 ( $\text{C=O}$ ) ppm.

FT-IR (neat): 2978 (C-H), 1723 (C=O), 1629 (C=C), 721 (C-Br)  $\text{cm}^{-1}$

### 3.2.5. Synthesis of *tert*-butyl 3,3-bis(diethoxyphosphoryl)propanoate

To a solution of tetraethyl methylenebisphosphonate (3.00 g, 10.4 mmol) in dry DMF (9 mL) was added 0.69 g of NaH (60% suspension in mineral oil, 17.25 mmol) portionwise. The resulting slurry was stirred for 30 min at room temperature, after which *tert*-butyl bromoacetate (1.7 mL, 11.5 mmol) was added neat and at a rapid pace. The reaction mixture was stirred for 1 h and quenched by adding 2 mL of a saturated solution of  $\text{NH}_4\text{Cl}$ . The reaction mixture was evaporated and *tert*-butyl 3,3-bis(diethoxyphosphoryl)propanoate was obtained as a yellow liquid in 58 % yield.

$^1\text{H-NMR}$  ( $\text{CDCl}_3$ ): 1.31 (t, 12 H,  $\text{CH}_2\text{CH}_3$ ), 1.44 (s, 9 H,  $\text{C}(\text{CH}_3)_3$ ), 2.75 (t, 2H,  $\text{CH}_2\text{CHP}_2$ ), 3.05 (t, 1H,  $\text{CHP}_2$ ), 4.16 (m, 8H,  $\text{OCH}_2\text{CH}_3$ ) ppm.

FT-IR (neat): 2921 (C-H), 1731 (C=O), 1255 (P=O), 1156 and 967 (P-O-Et)  $\text{cm}^{-1}$ .

### 3.2.6. Synthesis of 3,3-bis(diethoxyphosphoryl)propanoic acid

*tert*-butyl 3,3-bis(diethoxyphosphoryl)propanoate (2.1 g, 5.2 mmol) was stirred in TFA (12 mL) for 2.5 min and concentrated under reduced pressure. The acid derivative was obtained as liquid in 80 per cent yield.

<sup>1</sup>H-NMR (MeOD): 1.33(t, 12H, CH<sub>2</sub>CH<sub>3</sub>), 2.86 (t, 2H, CH<sub>2</sub>CHP<sub>2</sub>), 3.14(t, 1H, CHP<sub>2</sub>), 4.18 (m, 8H, OCH<sub>2</sub>CH<sub>3</sub>) ppm.

FT-IR(neat): 3484 (O-H), 1727 (C=O), 1203 (P=O), 1155 and 974 (P-O-Et)cm<sup>-1</sup>.

## 3.3. Synthesis of Bisphosphonated Methacrylates

### 3.3.1. Ethyl 2-((3,3-bis(diethoxyphosphoryl)propanoyloxy)methyl)acrylate

To a mixture of 3,3-bis(diethoxyphosphoryl)propanoic acid(0.485 g, 1.40 mmol) and K<sub>2</sub>CO<sub>3</sub> (0.193 g, 1.40 mmol) in MEK (3.50 mL), EBr (0.225 g, 1.17 mmol) was added. The mixture was stirred at 60 °C for 24 h under nitrogen atmosphere. After removal of the solvent, the mixture was diluted with 3 mL CH<sub>2</sub>Cl<sub>2</sub> and washed with brine (2x0.7 mL). The organic phase was dried with Na<sub>2</sub>SO<sub>4</sub>, filtered and the solvent was evaporated. The crude product was purified by column chromatography on silica gel 60 (70-230 mesh) using hexane initially and gradually changing to ethyl acetate as eluent. The pure product was obtained as light yellow oil in 28 % yield.

<sup>1</sup>H NMR (CDCl<sub>3</sub>): 1.34 (t, 15H, OCH<sub>2</sub>CH<sub>3</sub>), 2.92 (t, 2H, CH<sub>2</sub>CHP<sub>2</sub>), 3.11 (t, 1H, CHP<sub>2</sub>), 4.19 (m, 10H, OCH<sub>2</sub>CH<sub>3</sub>), 4.87 (s, 2H, CH<sub>2</sub>O), 5.89, 6.38 (s, 2H, C=CH<sub>2</sub>) ppm.

<sup>13</sup>C-NMR (CDCl<sub>3</sub>): 14.14 (CH<sub>3</sub>CH<sub>2</sub>OC), 16.83 (CH<sub>3</sub>CH<sub>2</sub>OP), 30.55 (CH<sub>2</sub>CHP<sub>2</sub>), 32.78 (CH<sub>2</sub>CHP<sub>2</sub>), 61.01 (CH<sub>2</sub>OC), 62.76 (CH<sub>2</sub>OP), 63.07 (CCH<sub>2</sub>O), 127.22 (CH<sub>2</sub>=C), 135.08 (CH<sub>2</sub>=C), 164.63 (CH<sub>3</sub>CH<sub>2</sub>OC=O), 170.39 (C=O) ppm

FT-IR: 2983 (C-H), 1740 (C=O), 1717 (C=O), 1640 (C=C), 1250 (P=O), 1155 and 962 (P-O-Et)cm<sup>-1</sup>.

### 3.3.2. *Tert*-butyl 2-((3,3-bis(diethoxyphosphoryl)propanoylox)methyl)acrylate

Monomer 2 was synthesized with the same procedure for monomer 1 using TBBBr instead of EBBBr. The pure product was also obtained by column chromatography as light yellow oil in 24 % yield.

$^1\text{H}$  NMR ( $\text{CDCl}_3$ ): 1.27 (t, 12H,  $\text{OCH}_2\text{CH}_3$ ), 1.44 (s, 9H,  $\text{C}(\text{CH}_3)_3$ ), 2.86 (t, 2H,  $\text{CH}_2\text{CHP}_2$ ), 3.05 (t, 1H,  $\text{CHP}_2$ ), 4.13 (m, 8H,  $\text{OCH}_2\text{CH}_3$ ), 4.77 (s, 2H,  $\text{CH}_2\text{O}$ ), 5.73, 6.21 (s, 2H,  $\text{C}=\text{CH}_2$ ) ppm.

$^{13}\text{C}$  NMR ( $\text{CDCl}_3$ ): 16.29 ( $\text{CH}_3\text{CH}_2\text{O}$ ), 27.97 ( $\text{C}(\text{CH}_3)_3$ ), 30.52 ( $\text{CH}_2\text{CHP}_2$ ), 32.74 ( $\text{CH}_2\text{CHP}_2$ ), 62.76 ( $\text{OCH}_2\text{CH}_3$ ), 63.14 ( $\text{CCH}_2\text{O}$ ), 81.38 ( $\text{C}(\text{CH}_3)_3$ ), 126.07 ( $\text{CH}_2=\text{C}$ ), 136.40 ( $\text{CH}_2=\text{C}$ ), 164.17 ( $\text{C}(\text{CH}_3)_3\text{OC}=\text{O}$ ), 170.31 ( $\text{C}=\text{O}$ ) ppm.

FT-IR (neat): 2978 (C-H), 1742 (C=O), 1717 (C=O), 1641 (C=C), 1252 (P=O), 1144 and 968 (P-O-Et)  $\text{cm}^{-1}$

## 3.4. Photopolymerizations

### 3.4.1. Photopolymerization Procedure

All the photopolymerizations were carried out on a TA Instrument Q 100 Photo-DSC equipped with a mercury arc lamp as the light source and using 2,2-dimethoxy-2-phenyl acetophenone (Irgacure 651) as the photoinitiator. The photoinitiator (~8 mg) was first dissolved in methylene dichloride (5 mL). 3-4 mg sample was placed in aluminum DSC pan. A methylene dichloride solution of the photoinitiator was added with a microsyringe to give a final concentration in the monomer of 2 mol per cent after evaporation of the solvent. The sample and the reference pans were placed in the DSC chamber, the system was purged with nitrogen flow to remove air and methylene dichloride for 10 min before polymerization and purging was continued during polymerization. The samples were irradiated for 10 min at 40  $^{\circ}\text{C}$  with an incident light intensity of 20  $\text{mW}/\text{cm}^2$ . The heat flow as a function of time was monitored using DSC under isothermal conditions and both the

rates of polymerization ( $R_p$ ) and degree of conversions were calculated as a function of time. The rates of polymerizations were calculated according to the following formula:

$$\text{Rate} = \frac{(Q/s)M}{n \Delta H_p m}$$

where  $Q/s$  is the heat flow per second,  $M$  is the molar mass of the monomer,  $n$  is the number of double bonds per monomer molecule,  $\Delta H_p$  is the heat released per mole of double bonds reacted and  $m$  is the mass of monomer in the sample. The theoretical value used for  $\Delta H_p$  was 13.1 kcal/mol for methacrylate double bonds [47,48].

### 3.5. Free Radical Polymerizations in Bulk and Solution

#### 3.5.1. Polymerization Procedure

3.5.1.2. Thermal Polymerizations The thermal homo- and copolymerizations were carried out with standard freeze-evacuate-thaw procedures

- (i) The homopolymerizations of monomers 1 and 2 were carried out in bulk at 65 °C with AIBN as initiator. The polymers were purified by precipitation into diethyl ether where monomers are soluble
- (ii) The copolymerizations of monomers 1 and 2 with PEGMA in three different ratios (one ratio) were carried out (2: PEGMA, 10:90, 30:70 and 50:50, 1: PEGMA 50:50) in methanol at 65 °C with AIBN as initiator. The copolymers were purified by precipitation into cold ether where both monomers are soluble.

### 3.6. Hydrolysis of a Copolymer

TMSBr (0.128g, 0.838 mmol) was added dropwise to a solution of the copolymer (2: PEGMA, 50:50 mol%) (0.2 g) in 0.6 mL dry dichloromethane under nitrogen. After 4 h of reflux, the solvent was removed under reduced pressure. The residue was diluted with 1.8 mL of methanol and the solution was stirred at room temperature overnight. After evaporation of methanol, the polymer was obtained as a solid in 85% yield.

### 3.7. Acidity and Interaction of Hydrolyzed Copolymer (2:PEGMA, 50:50 mol%) with Hydroxyapatite

The pH value of aqueous solution of the hydrolyzed polymer with and without HAP was measured. FT-IR spectrum of the copolymer (2:PEGMA, 50:50 mol%) with and without HAP were obtained. 0.1 g of copolymer (2:PEGMA, 50:50 mol%) was dissolved in 1.9 g of 5 wt % H<sub>2</sub>O. To this solution, 15 mg of HAP was added. After the suspension was stirred at 37 °C for 1h, the pH value was measured and FT-IR spectrum analysis was performed. Then another 15 mg of HAP was added to the solution and the same procedure was repeated again.

## 4. RESULTS AND DISCUSSION

### 4.1. Monomer Synthesis and Characterization

We synthesized two novel bisphosphonate-containing monomers, where the bisphosphonate groups are attached to double bond through an ester link.

Synthesis of these bisphosphonate-containing monomers involved three steps: i) monoalkylation of the sodium carbanion of tetraethylmethylene bisphosphonate in dry DMF with *tert*-butyl bromoacetate giving the first intermediate (*tert*-butyl 3,3-bis(diethoxyphosphoryl)propanoate) in 57 % yield, (ii) straightforward conversion of this intermediate to the carboxylic acid (*tert*-butyl 3,3-bis(diethoxyphosphoryl)propanoic acid) by cleavage of *tert*-butyl groups using trifluoroacetic acid in 80 % yield, iii) reaction of the carboxylic acid with EBBr or TBBr in the presence of  $K_2CO_3$  in MEK at 60 °C (Figure 4.1.). The crude products were purified by column chromatography and the pure products were obtained as light yellow oils in 28 and 24 % yield, respectively. The monomers were soluble in common organic solvents such as methylene chloride, acetone, ether, methanol and THF but insoluble in water and hexane (Table 4.1).

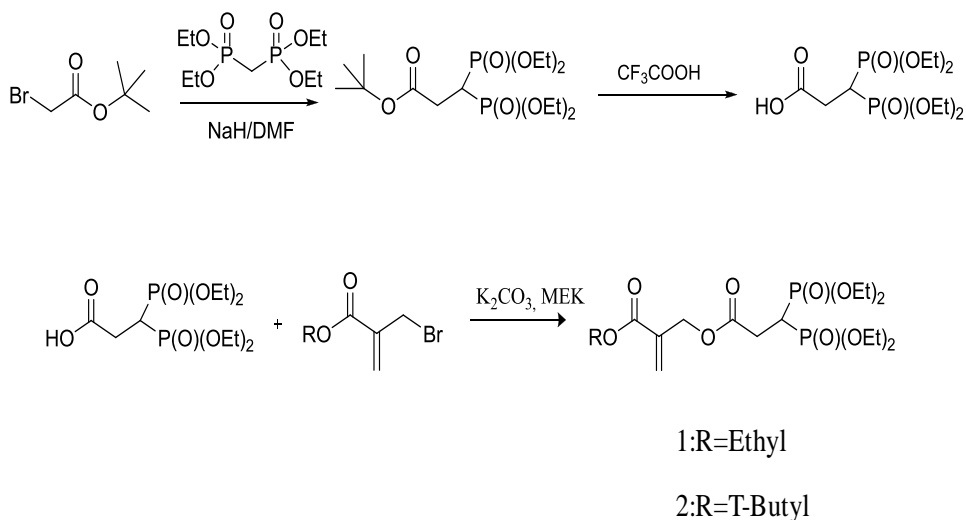


Figure 4.1. Synthesis of monomers 1 and 2.

Table 4.1. Solubility of Monomers and Polymers.

Monomer/Polymers	H <sub>2</sub> O	Methanol	Acetone	CH <sub>2</sub> Cl <sub>2</sub>	THF	Ether	Hexane
1	-	+	+	+	+	+	-
2	-	+	+	+	+	+	-
Poly-1	+	+	+	+	+	-	-
Poly-2	+	+	+	+	+	-	-

The characterization of the novel monomers was carried out by <sup>1</sup>H, <sup>13</sup>C NMR and by FTIR spectroscopies and the data obtained are in agreement with the expected monomer structures. <sup>1</sup>H NMR spectrum of the first intermediate during synthesis of monomer 2 demonstrated methyl and *tert*-butyl peaks at around 1.31 and 1.44 ppm and methylene protons at 2.75 and 4.16 ppm and a methine proton at around 3.05 ppm (Figure 4.2). In the second spectrum, the complete disappearance of *tert*-butyl peak was observed after hydrolysis. Finally, <sup>1</sup>H NMR spectrum of monomer 2 showed methyl and *tert*-butyl peaks at around 1.27 and 1.44 ppm, three different methylenes at 2.86, 4.13 and 4.77 ppm and double bond peaks at 5.73 and 6.21 ppm (Figure 4.2). In the <sup>1</sup>H NMR spectrum of monomer 1, the single bisphosphonate proton is supported by the presence of a triplet at 3.11 ppm. The <sup>13</sup>C NMR spectrum of monomer 2 showed characteristic peaks for methyl carbons at 16.29 and 27.97 ppm, a tertiary carbon attached to phosphorus at 30.52 ppm, double bond carbons at 126.07 and 136.40 ppm and two carbonyl carbons at 164.17 and 170.31 ppm (Figure 4.3).

FTIR spectra of monomers 1 and 2 showed peaks due to two different C=O, C=C, P=O and P-O peaks at around 1740 and 1720, 1640, 1255, 1020 and 960 cm<sup>-1</sup> (Figure 4.4).

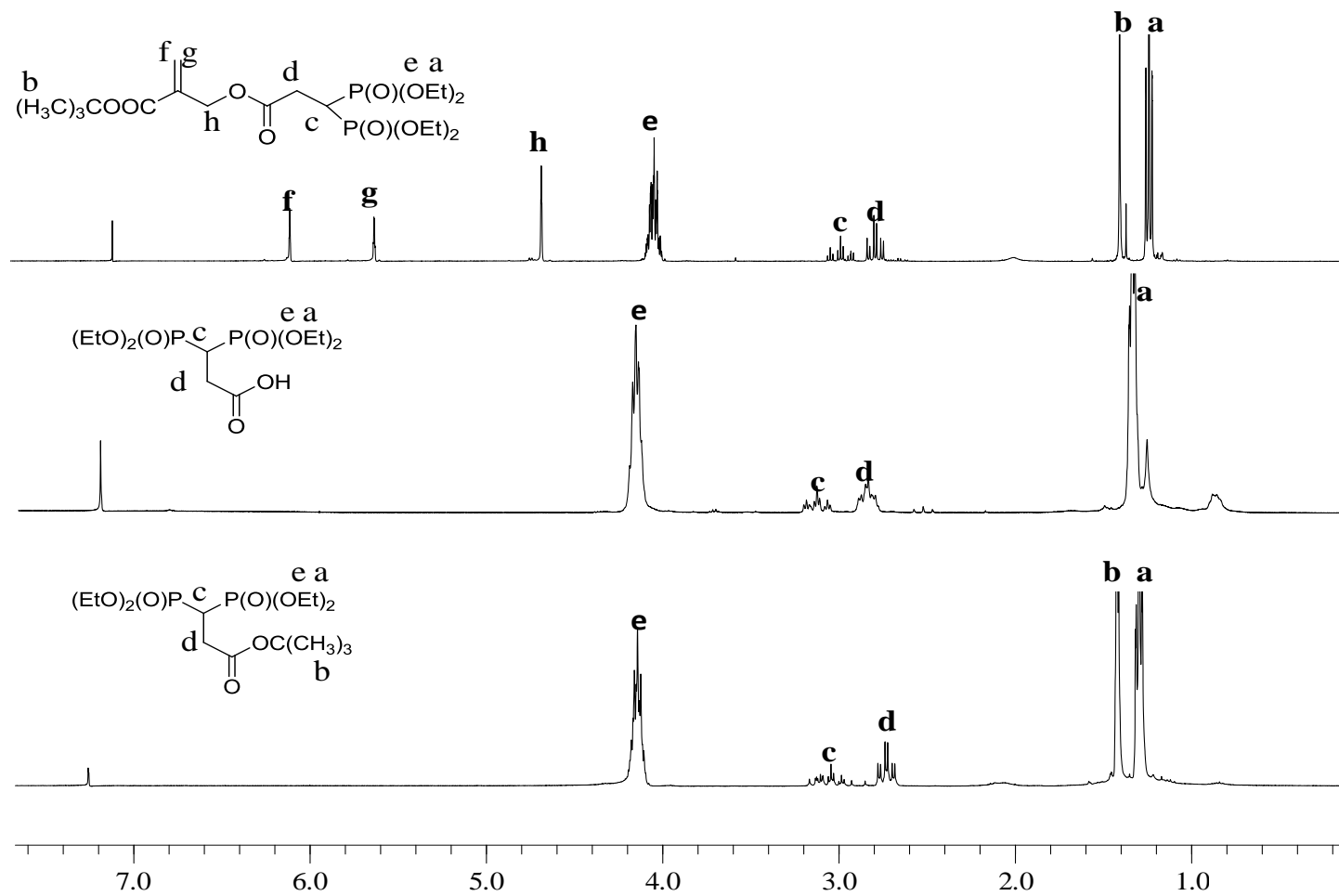


Figure 4.2.  $^1\text{H}$  NMR spectra of monomer 2 and intermediate compounds.

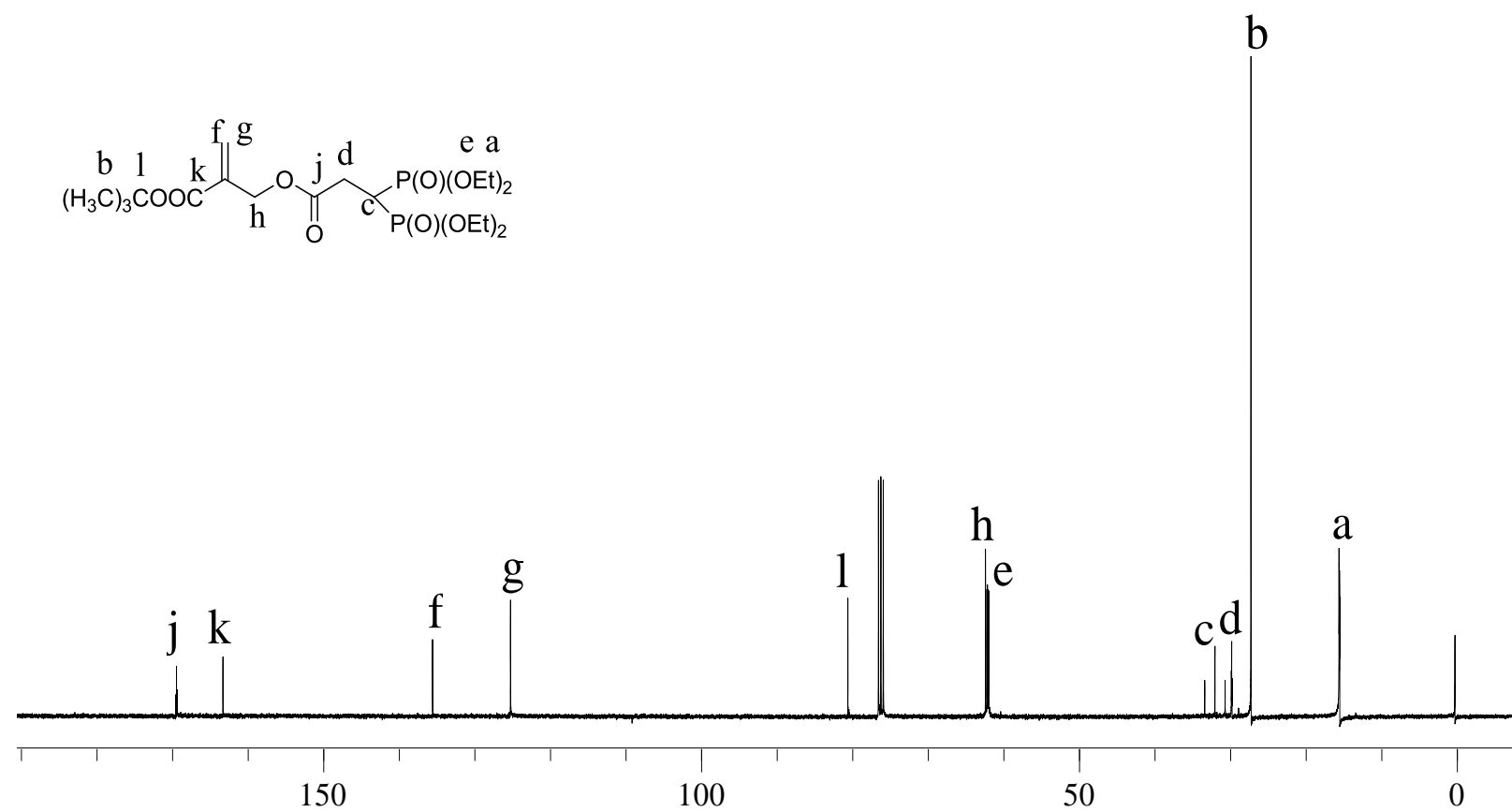


Figure 4.3.  $^{13}\text{C}$  NMR spectrum of monomer2.

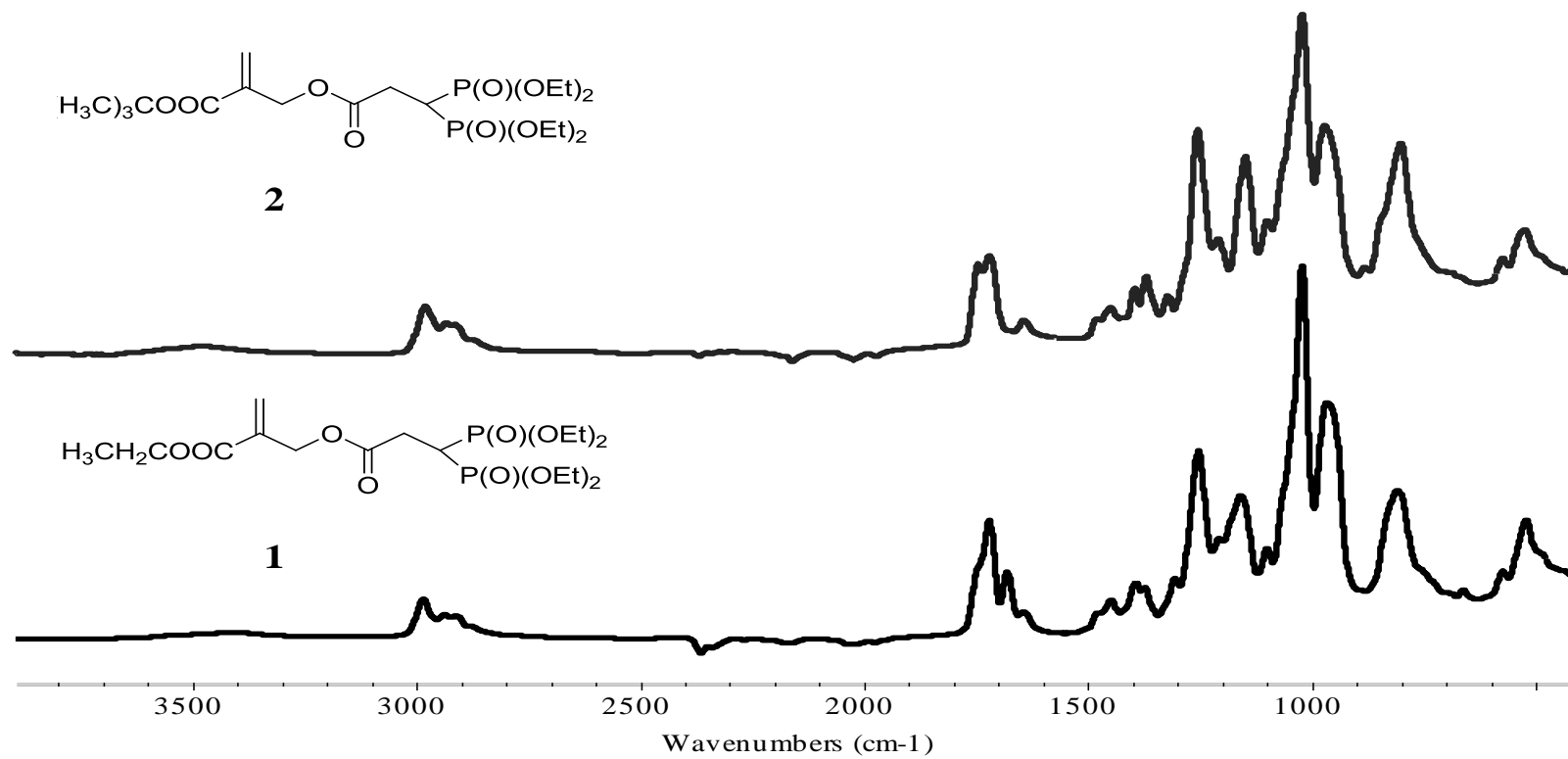


Figure 4.4. FTIR spectra of monomer 1 and 2.

## 4.2. Homopolymerizations

Thermal bulk polymerizations of monomers were carried out using AIBN and standard freeze-evacuate-thaw procedures at 65 °C. The polymerization conditions and the characteristics of the polymers are listed in Table 4.2. The results showed that the conversions reached for monomer 1 and 2 were 23 and 25% in 300 min. These low conversions may be due to chain transfer reactions from the labile hydrogen between two phosphonate groups in the monomers structure.

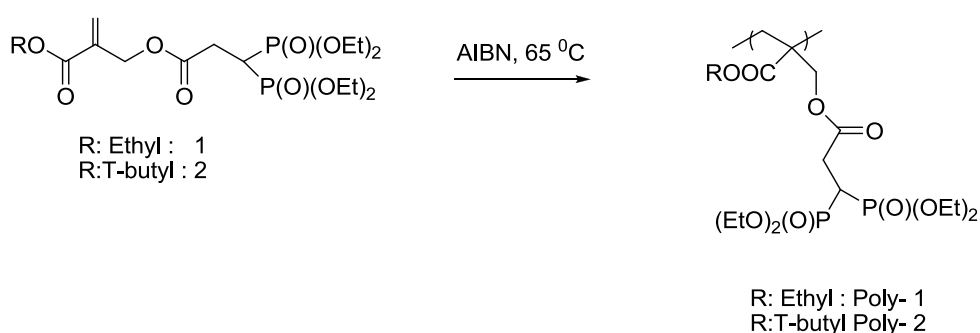


Figure 4.5. Polymerization of monomer 1 and 2.

Polymers of 1 and 2 were obtained as white solids after precipitation into cold ether where both monomers are soluble. These polymers were found to be soluble in weakly polar organic solvents such as acetone, methylene chloride and THF and also soluble in polar solvents such as methanol and water due to their highly polar structures. Figure 4.6 shows  $^1\text{H}$  NMR spectrum of poly-1 without any trace of unreacted monomer. The GPC analysis indicated that the polymers have molecular weights of 83000 and 59500 for poly-1 and poly-2, indicating the effect of bulky *tert*-butyl group.

Table 4.2. Thermal Homo- and Copolymerization of the Bisphosphonate monomers with PEGMA( $M_n=950$  g/mol).

Monomer <sup>a)</sup>	Bisphosp. Mon.in feed [mol %]	Bisphosp. Mon. in copolymers <sup>b)</sup> [mol%]	Solvent	AIBN [wt %]	Time [min]	Yield [%]	$M_n$
1	100	-	Bulk	1.5	300	23	83000
1	50	38	MeOH	1.5	120	35	15000
2	100	-	Bulk	1.5	300	25	59500
2	50	31	MeOH	1.5	120	37	10000
2	30	- <sup>c)</sup>	MeOH	1.5	12	25	33000
2	10	-	MeOH	1.5	7	Crosslinked	-

<sup>a)</sup>  $[M]= 2.2$  M.

<sup>b)</sup> Determined by  $^1\text{H}$  NMR.

<sup>c)</sup> Undetermined due to peak overlap in  $^1\text{H}$  NMR spectrum

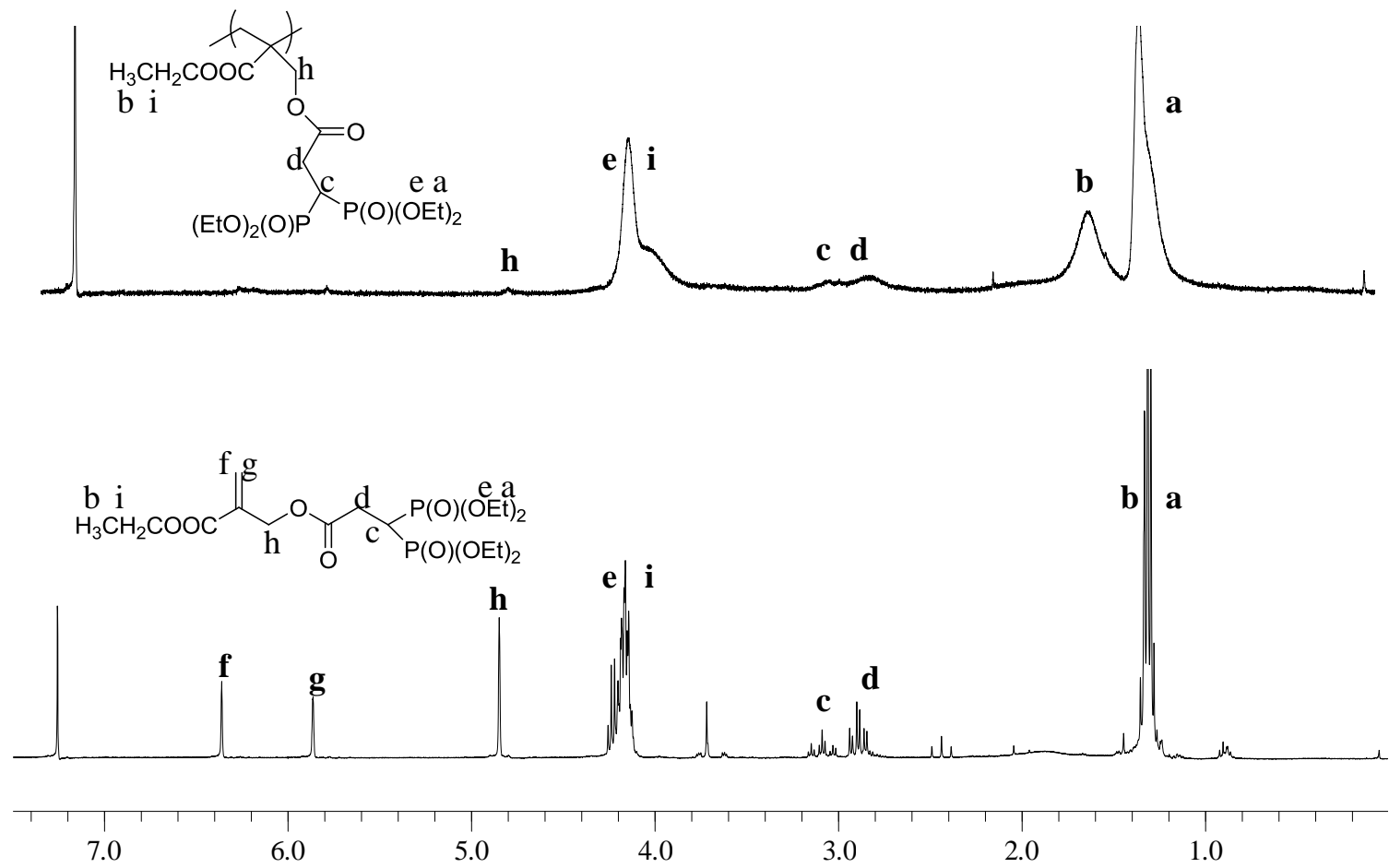


Figure 4.6.  $^1\text{H}$  NMR spectra of monomer 1 and poly-1.

The glass transition temperatures ( $T_g$ ) of poly-1 and poly-2 were found to be 75 and 85 °C. The relatively high  $T_g$  of poly-2 compared to poly-1 can be explained by the bulky *tert*-butyl groups.

### 4.3. Copolymerizations

We also prepared water soluble copolymers of 1 and 2 with PEGMA, a universal polymer used for drug delivery due to its biocompatible and nonimmunogenic nature (Figure 4.7) [28]. Although several PEGMA derivatives with different molecular weights and end groups are available commercially, we used the one with methoxy end group due to facile detection by  $^1\text{H}$  NMR. The copolymerization of the synthesized monomers (1 and 2) with PEGMA ( $M_n=950$  g/mol) was performed at 65 °C using AIBN as initiator.

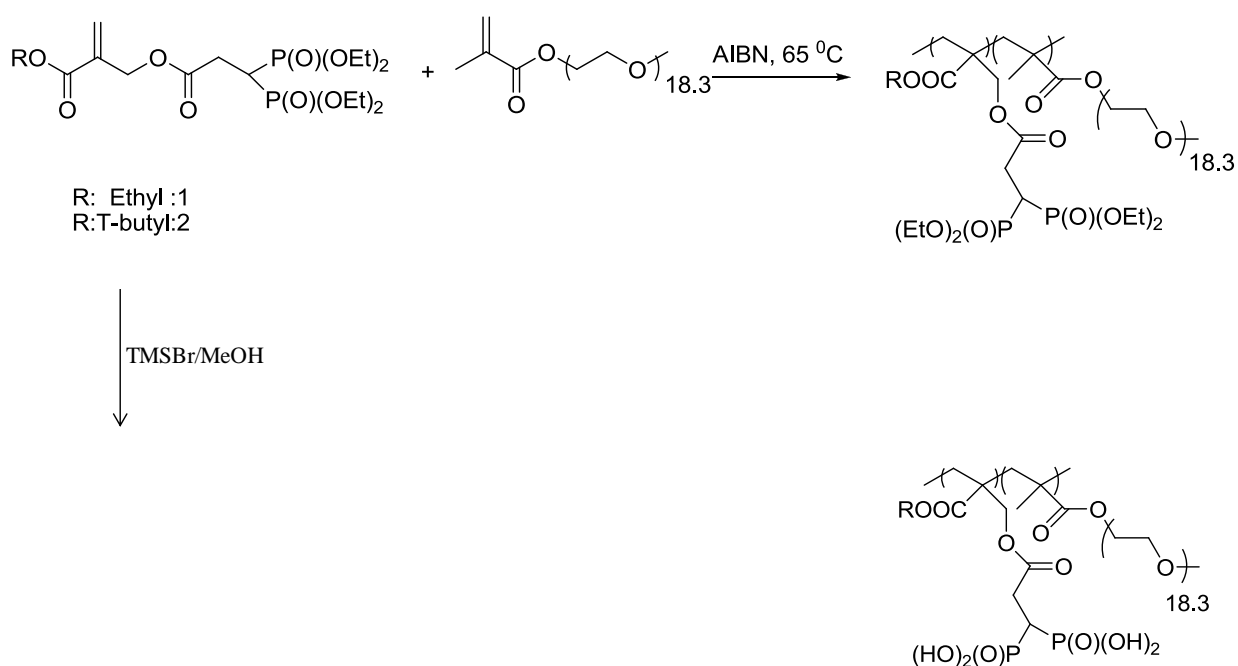


Figure 4.7. Copolymerization of monomers with PEGMA.

Bulk copolymerization studies mostly resulted in crosslinked polymers in a very short time, similar to homopolymerization of PEGMA. Therefore, solution polymerizations in methanol were carried out and the soluble polymers were purified by precipitation into cold ether after a selected period of time. The concentration of bisphosphonate monomer in

feed ratio was 10, 30 and 50 mol %. The obtained polymers were white powders. It was observed that as the concentration of PEGMA in feed ratio increased, the rate of polymerization and the crosslinking tendency of the copolymerization system increased (Table 4.2). During copolymerizations of 2 with PEGMA soluble copolymers were obtained at 70:30 and 50:50 mol % feed ratios. This result is expected due to higher reactivity of PEGMA (maximum rate of photopolymerization =  $0.013 \text{ s}^{-1}$ , conversion = 93%) compared to bisphosphonate-containing monomers observed from photo-DSC experiments which will be mentioned in the photopolymerization part in detail. To compare, PEGMA homopolymerization was carried out in methanol but at much lower monomer concentrations (0.6 M) and a soluble polymer was obtained with a  $M_n$  value of 235000. The lower molecular weight of the copolymers (10000-33000) is due to chain transfer ability of the synthesized monomers.

The copolymer compositions were determined from the integrated  $^1\text{H}$  NMR spectra of the copolymers. Figure 4.8 shows  $^1\text{H}$  NMR of one of the copolymers (PEGMA: 2, 50:50 mol% in feed). The peaks at 3.38 and 3.60-3.90 ppm are due to the methoxy protons ( $-\text{OCH}_3$ ) and methylene protons ( $-\text{OCH}_2\text{CH}_2-$ ) of PEGMA. Methyl protons of PEGMA and 2 and backbone protons overlap at 0.8-1.6 ppm. The peak at around 4.0 ppm is assigned to methylene protons of 2 and PEGMA adjacent to oxygen. Integration of this peak relative to methoxy protons of PEGMA (3.38 ppm) showed PEGMA: 2, 69:31 mol %. The structure of the copolymer was also confirmed by the FTIR spectra (Figure 4.9). The strong stretching band at around  $1100 \text{ cm}^{-1}$  originates from the characteristic ether linkage ( $-\text{CH}_2-\text{O}-\text{CH}_3$ ) of PEGMA. The DSC curves of poly-PEGMA, and all of the copolymers obtained showed one melting endotherm which indicate the melting of PEG.

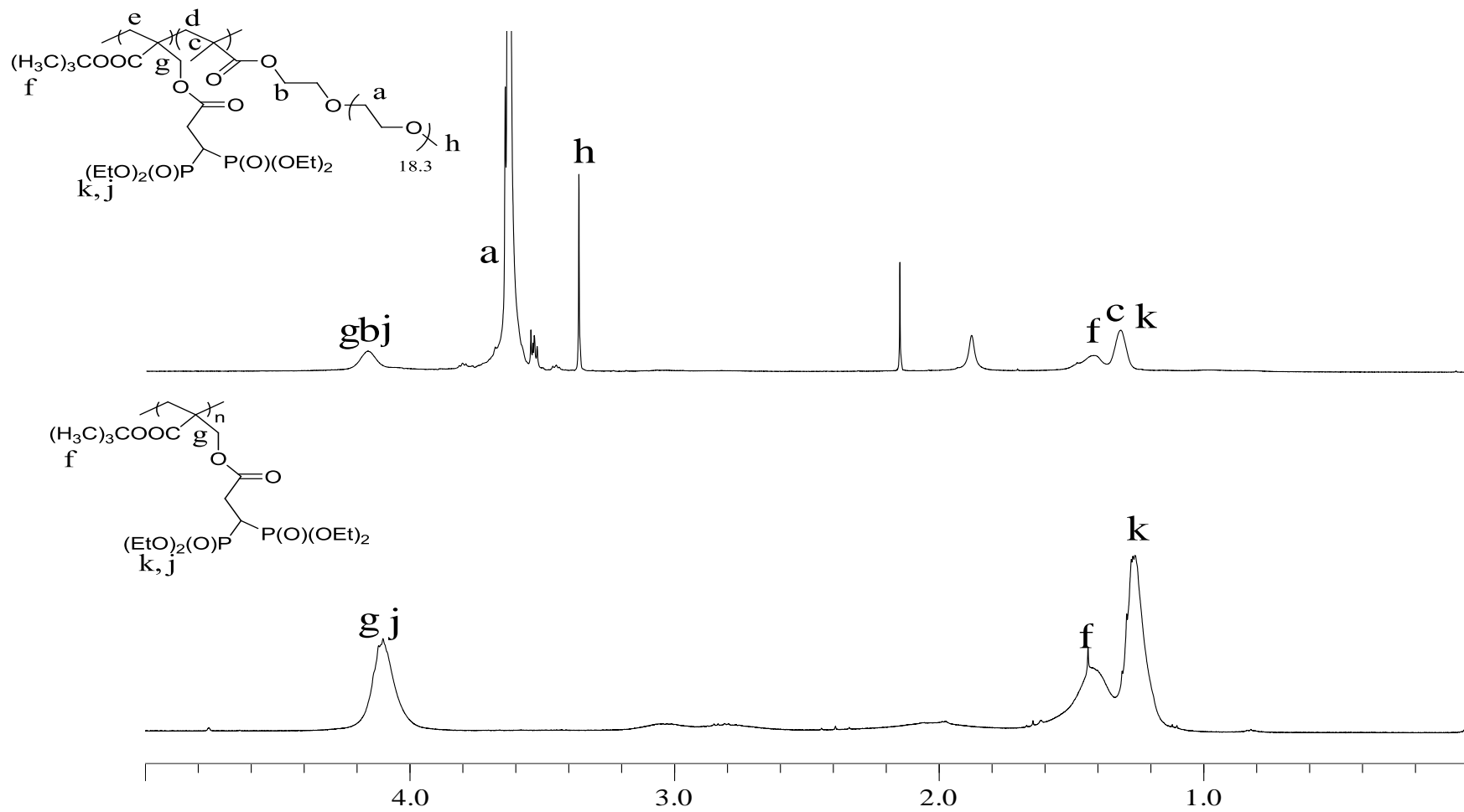


Figure 4.8.  $^1\text{H}$  NMR spectra of poly-2 and 2:PEGMA (50:50 mol%) copolymer.

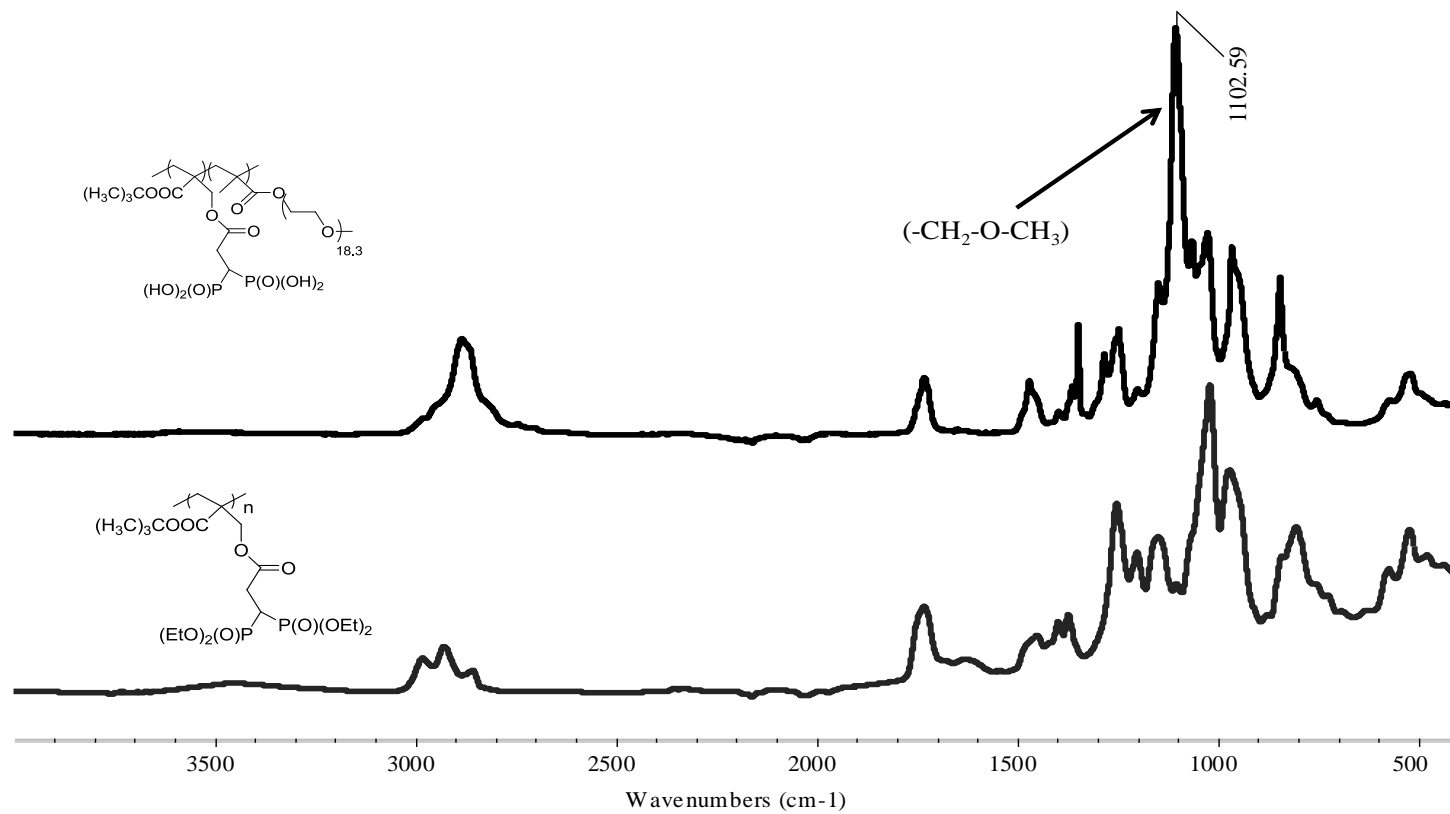


Figure 4.9. FTIR spectra of poly-2 and 2:PEGMA (50:50 mol%) copolymer.

To further evaluate the reactivities of these monomers in free-radical polymerizations, they were photopolymerized with 2 mol % DMPA with photo-DSC. All the polymerizations were performed under identical conditions of temperature, initiator concentration and light intensity. Figure 4.10 shows the time dependences of the polymerization rate and conversions for monomers. In earlier work, it was observed that increasing the size of the ester group from ethyl to *tert*-butyl decreases the polymerization rate because of steric hindrance [49]. However, monomer 1 showed less reactivity/conversion than expected. We are unable to explain this behaviour; one possibility is the presence of an impurity. The conversions were 44 and 64 % for monomers 1 and 2, respectively, and they were reached in about 6 min.

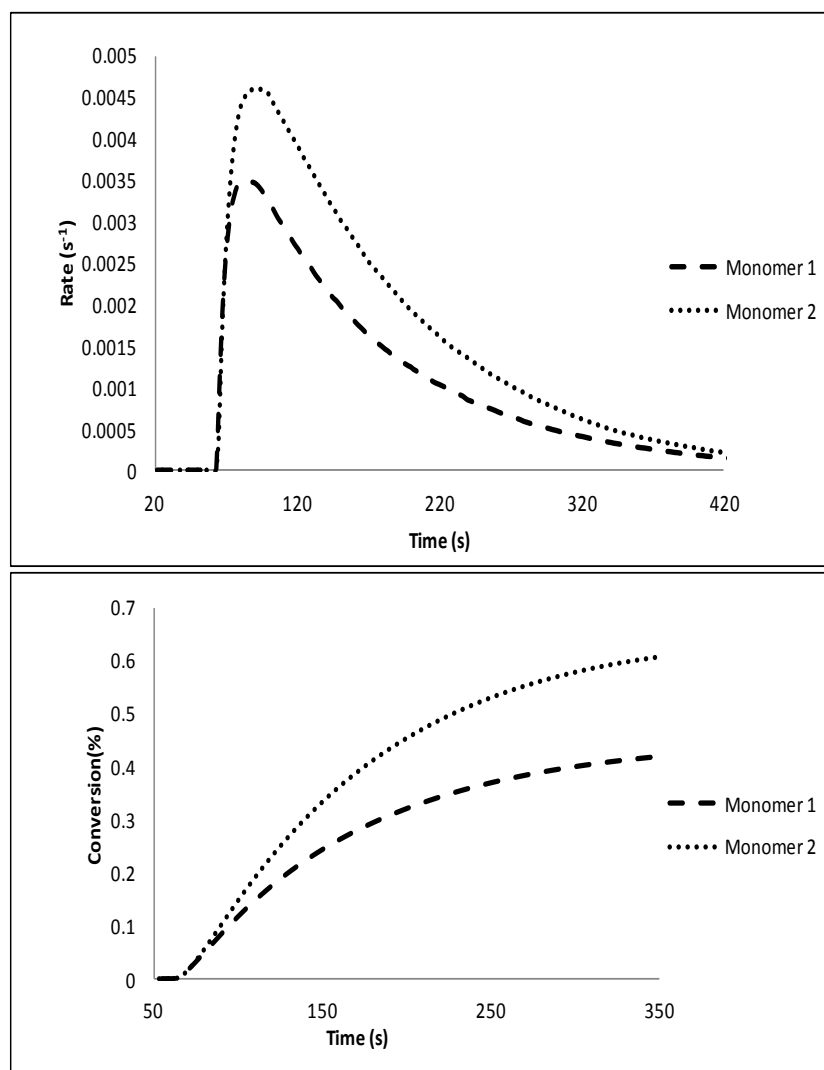


Figure 4.10. Rate-time and conversion-time curves in the polymerizations of 1 and 2.

In order to test the use of these monomers in dental adhesives and filling composites, we investigated copolymerization of them with HEMA which is an important, commercial monomer in dental applications. Figure 4.11 shows the result of the copolymerization of monomer 2 with HEMA. The rate and conversion of HEMA were found to be higher than monomer 2. This behavior was expected because hydrogen bonding in HEMA is a rate enhancing factor. Also, bulky *tert*-butyl group in monomer 2 is decreasing both the rate and conversion due to steric hindrance. Therefore, addition of 30 and 50 mol % of monomer 2 to HEMA decreased its rate. Additionally, the results clearly show that there is a shift in the peak maximum of monomer 2 by the addition of HEMA which confirms the incorporation of the synthesized monomers into the copolymers.

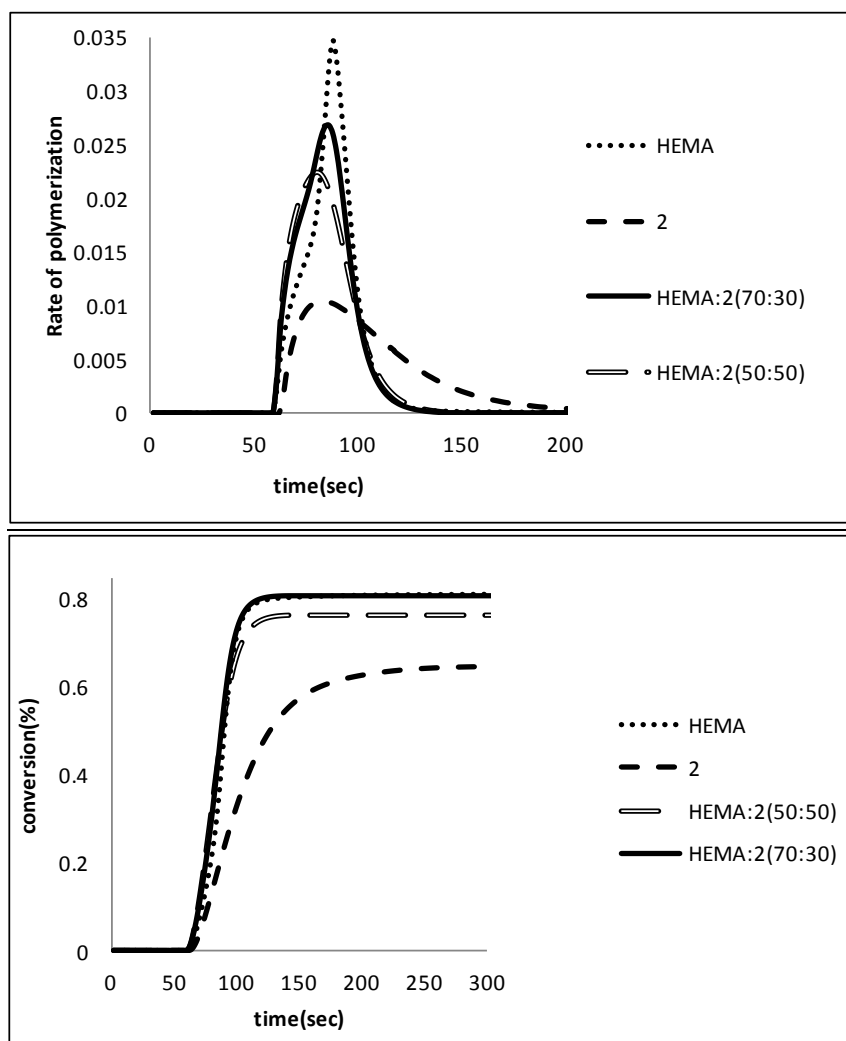


Figure 4.11. Rate-time and conversion-time curves in the polymerizations of 2 and 2:HEMA (30-70 mol %), 2:HEMA (50-50 mol %) HEMA.

#### 4.4. Hydrolysis of Polymers

The bisphosphonate groups of the copolymer of 2 with PEGMA (50:50 mol% feed ratios) were hydrolyzed using TMSBr. The hydrolysis was verified by  $^1\text{H}$  NMR spectra in which the integration of ethyl peaks (at around 1.20 and 4.00 ppm) decreased with respect to other peaks (Figure 4.12). The FTIR spectrum of the hydrolyzed copolymer showed broad peaks in the region of  $3500\text{-}2600\text{ cm}^{-1}$  due to OH stretching and peaks at around  $1700$  and  $1100\text{ cm}^{-1}$  due to C=O and P=O stretchings. Also the bands at  $1020$  and  $940\text{ cm}^{-1}$  correspond to the symmetric and asymmetric vibration of P-O. In the DSC study, the hydrolyzed copolymer showed only melting of PEGMA.

#### 4.5. Acidity and Interactions with HAP

The pH value of the aqueous solution of the hydrolyzed copolymer 2: PEGMA (50:50 mol%) (5 wt %) was found to be 1.89. HAP, a model compound for bone, was added to the solution of the hydrolyzed copolymer and stirred at  $37\text{ }^\circ\text{C}$  for 1 h. After addition of 30 mg HAP and stirring for another 1 h at  $37\text{ }^\circ\text{C}$ , a quite different FTIR spectrum from that of the pure polymer was obtained. A slight shift of P-O stretching vibration of the copolymer from  $1095$  to  $1083\text{ cm}^{-1}$  upon mixing with HAP may indicate interaction of the copolymer with the latter. The peaks at  $1016$  and  $560\text{-}600\text{ cm}^{-1}$  originates from the phosphate group of HAP (Figure 4.13).

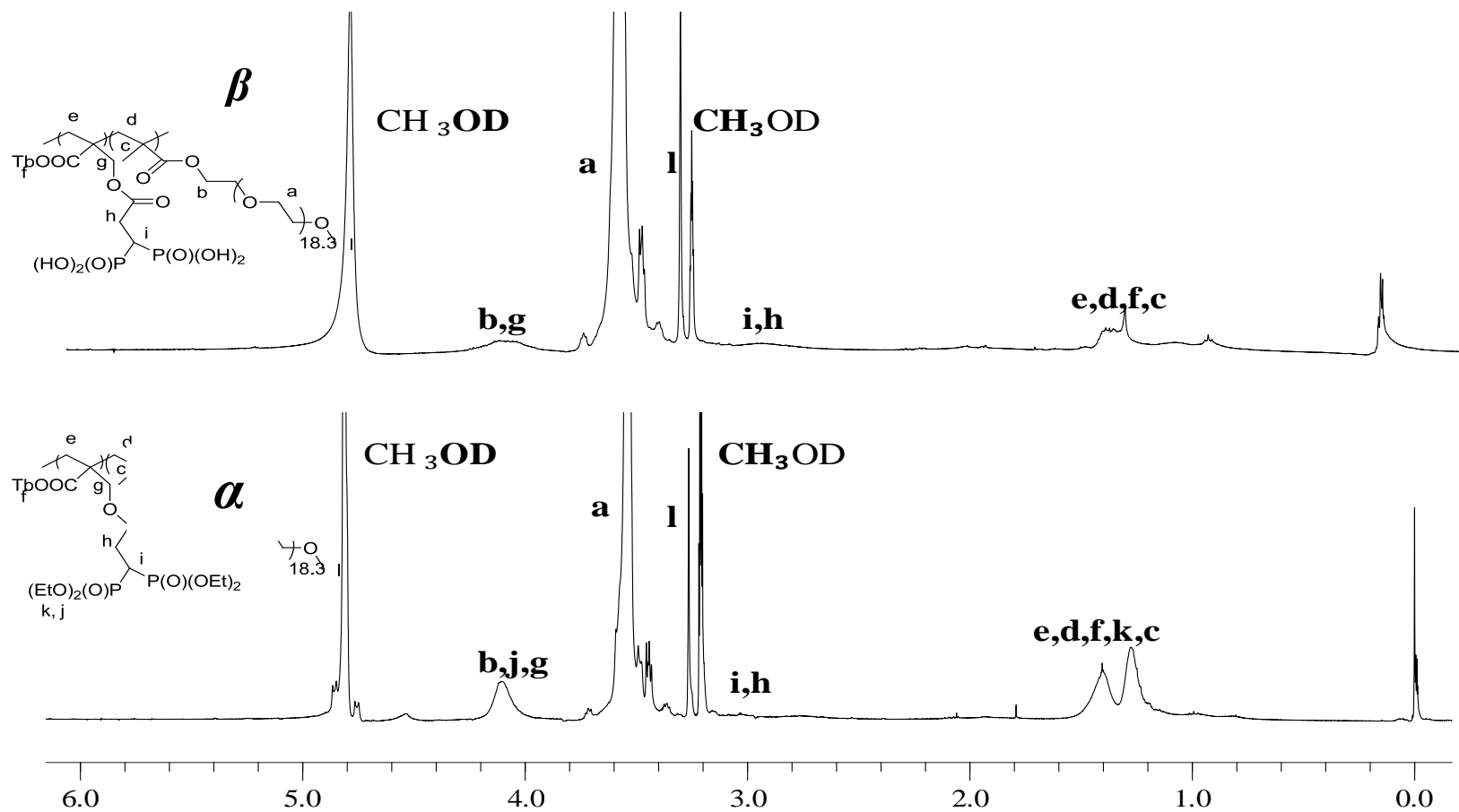


Figure 4.12. <sup>1</sup>H NMR spectra of 2: PEGMA (50:50 mol %) copolymer ( $\alpha$ ) and hydrolyzed 2:PEGMA (50:50 mol%) copolymer ( $\beta$ ).

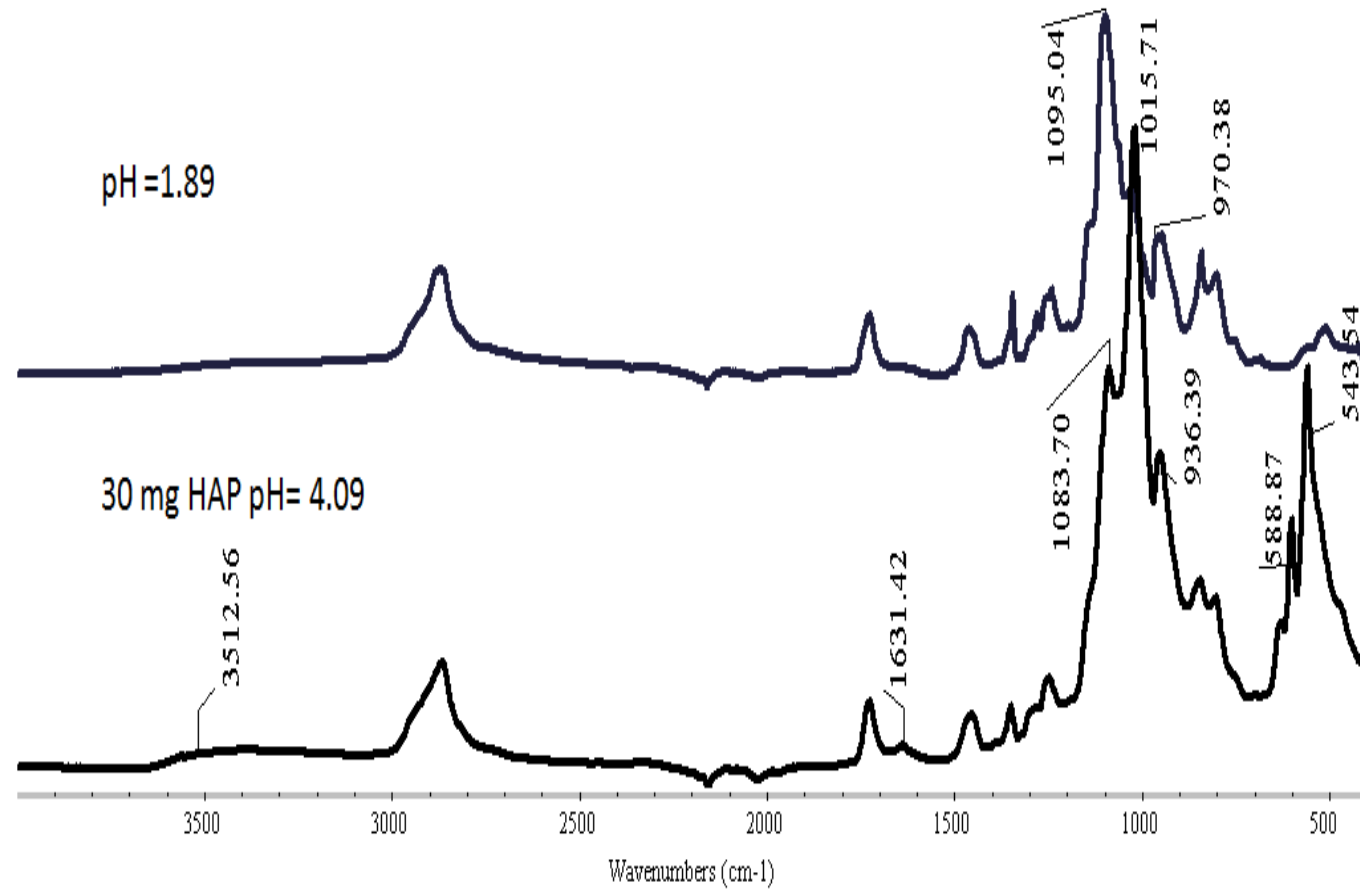


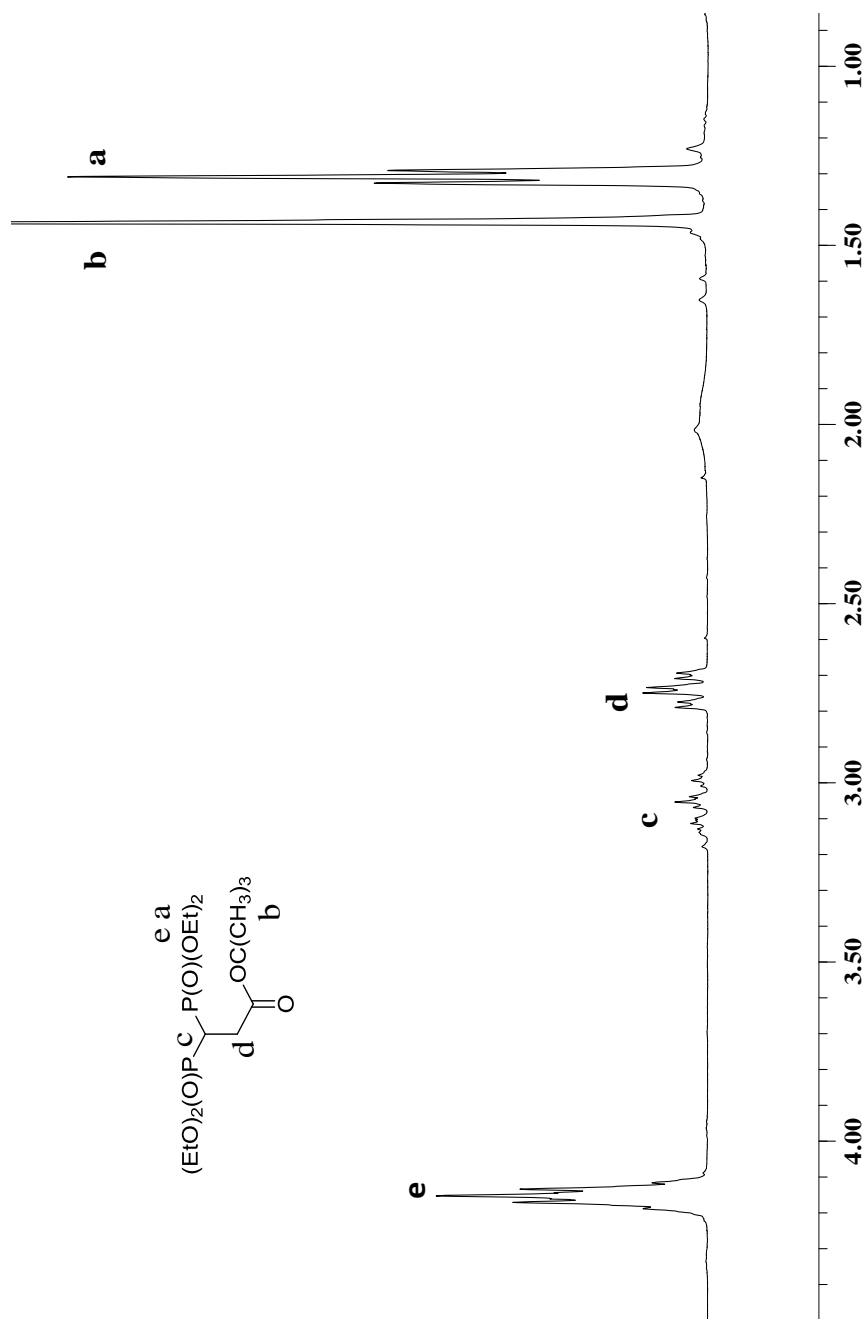
Figure 4.13. FTIR spectra of hydrolyzed copolymer 2: PEGMA(50:50 mol%) with 30 mg HAP.

## 5. CONCLUSION

Two new RHMA derivatives (monomers 1 and 2) carrying a bisphosphonate moiety were successfully synthesized. Radical homo- and copolymerizations of these monomers with PEGMA were carried out to obtain bisphosphonate-containing polymers. The results indicated good homopolymerization (20-25 % in thermal and 40-60% in photopolymerizations) and good copolymerization tendencies with PEGMA. Bisphosphonate groups of one of the copolymers were hydrolyzed to give a new bisphosphonic acid-containing polymer and the interaction of this copolymer with HAP was investigated. These polymers may have potential to be used as biomaterials. Future work will be the deprotection of bisphosphonate groups of the monomers to obtain new self-etching adhesive monomers.

## APPENDIX A: SPECTROSCOPY DATA

Figure A.1.  $^1\text{H}$  NMR spectra of 3,3-bis(diethoxyphosphoryl)propanoate in  $\text{CDCl}_3$ .



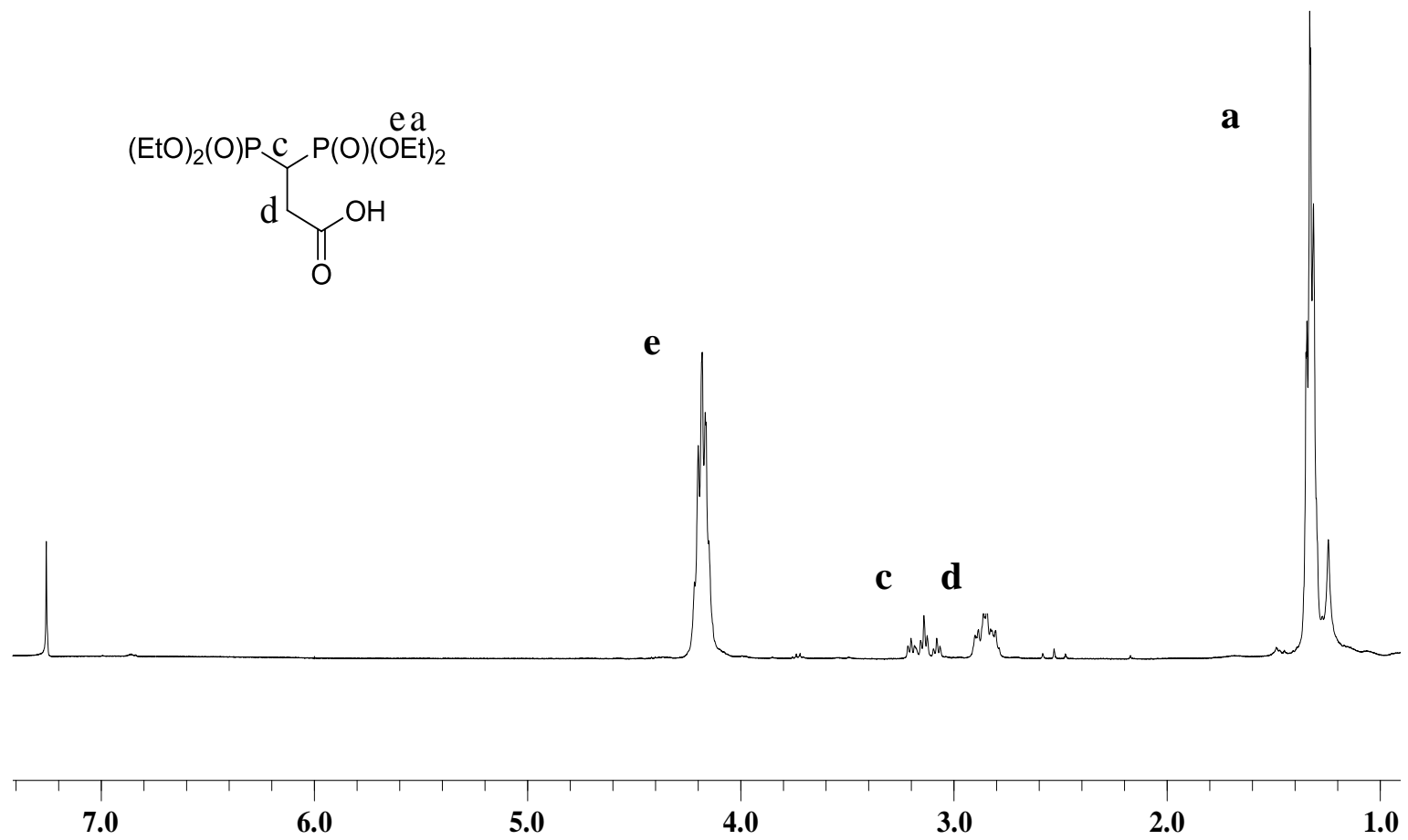


Figure A.2. <sup>1</sup>H NMR spectra of 3,3-bis(diethoxyphosphoryl)propanoic acid in CDCl<sub>3</sub>.

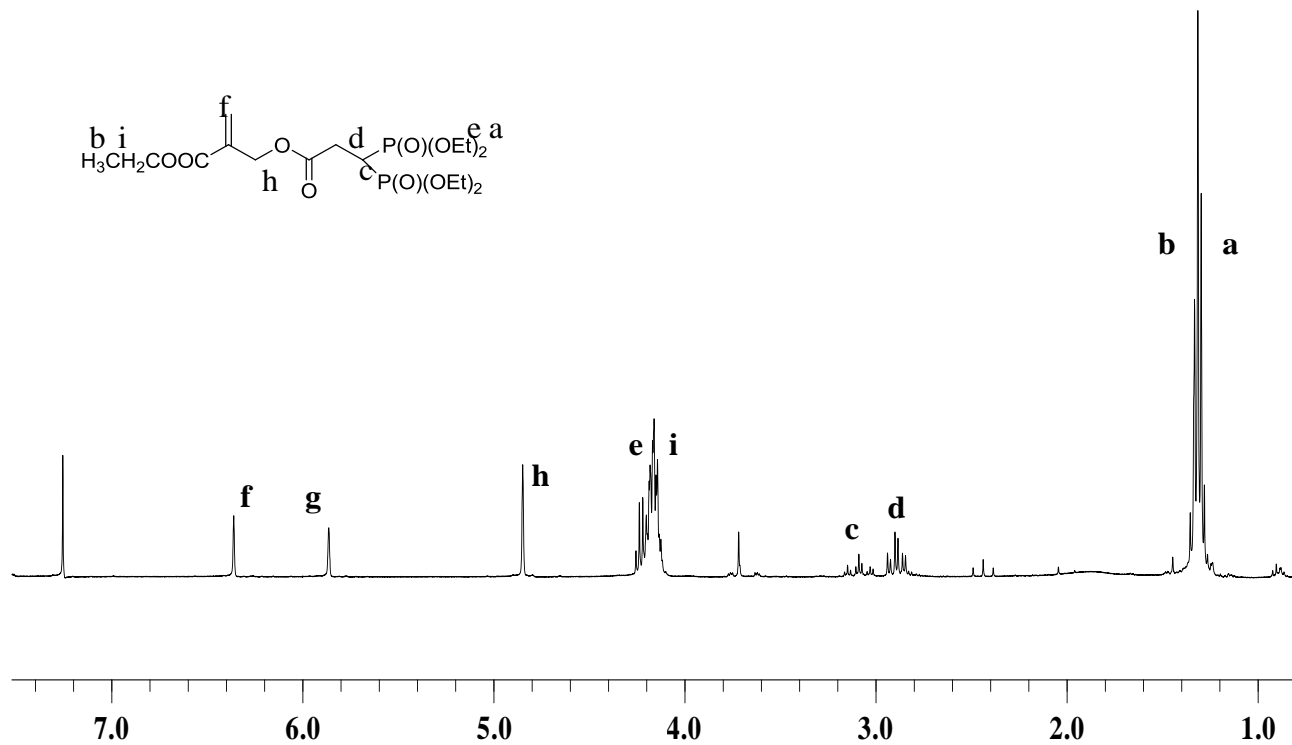


Figure A.3.  $^1\text{H}$  NMR spectra of monomer 1 in  $\text{CDCl}_3$ .

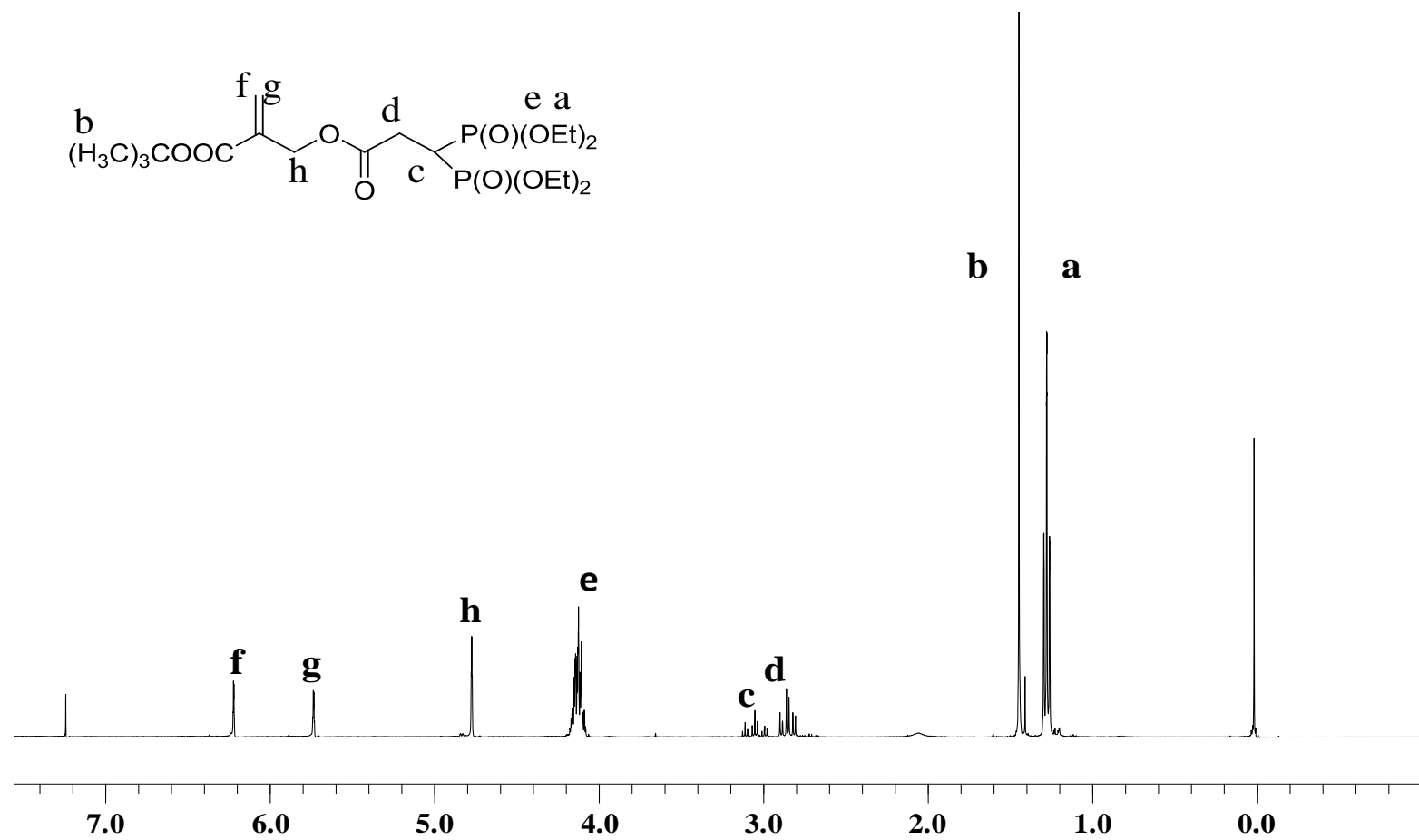


Figure A.4.  $^1\text{H}$  NMR spectra of monomer 2 in  $\text{CDCl}_3$ .

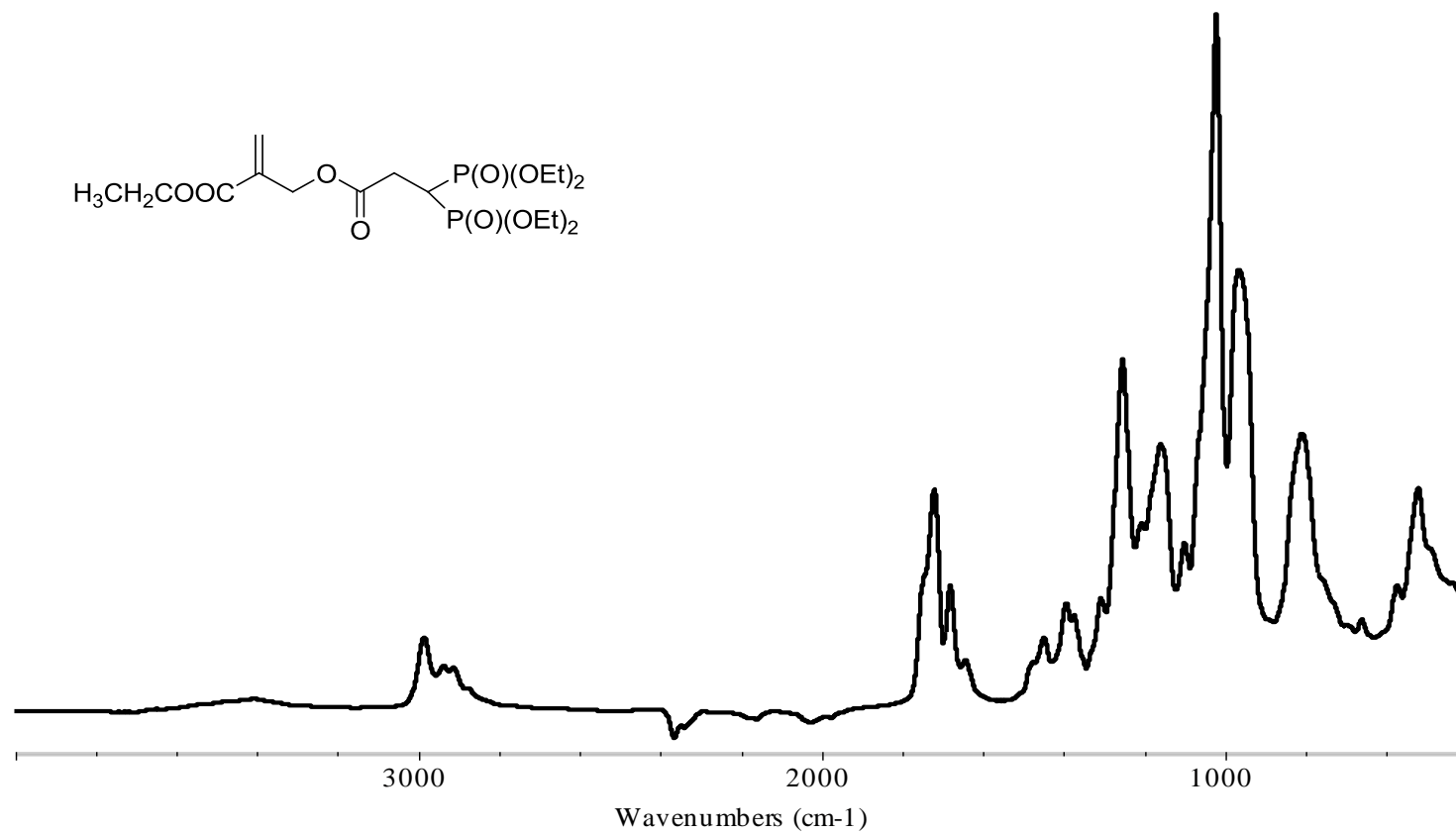


Figure A.5. FTIR spectrum of monomer 1.

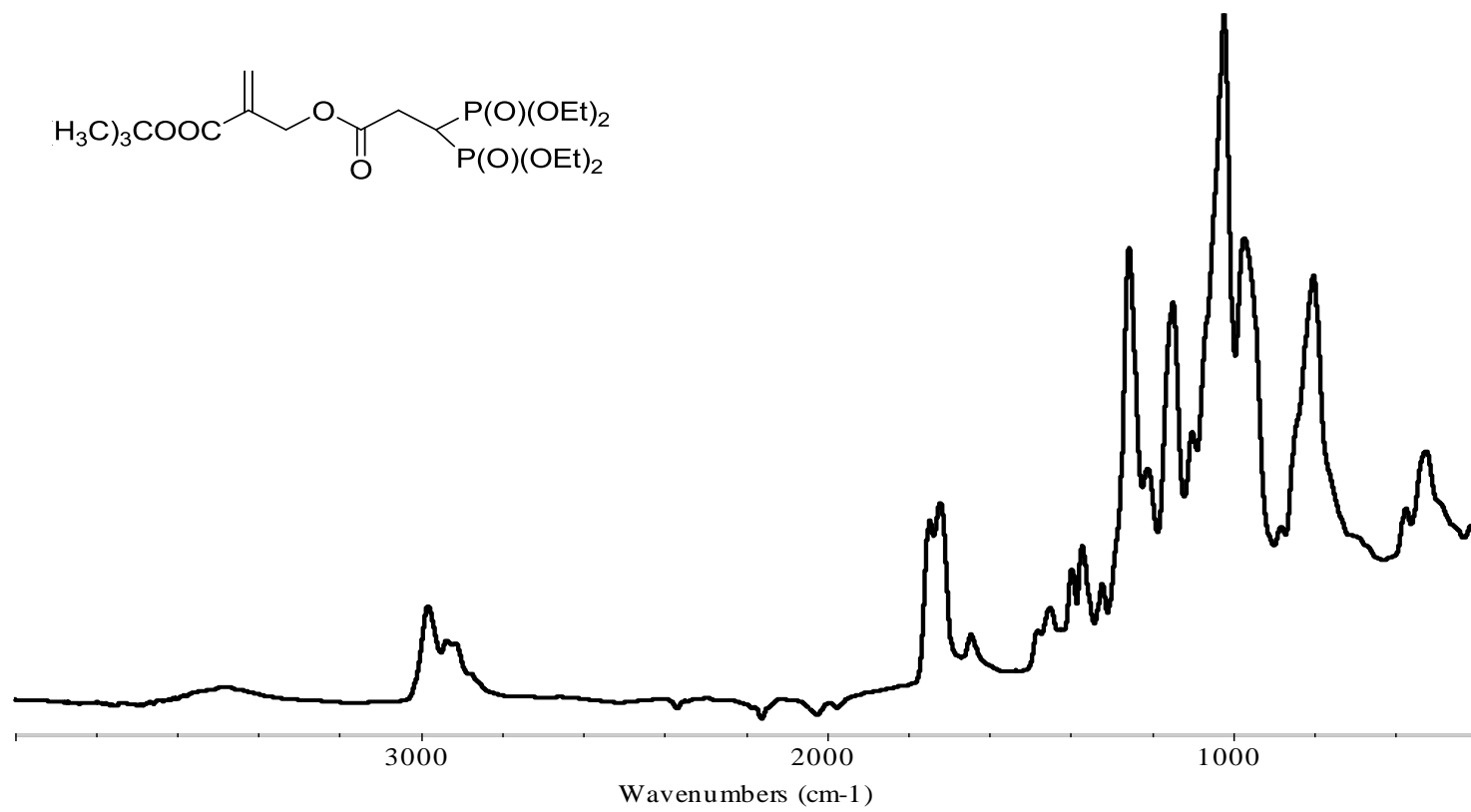


Figure A.6. FTIR spectrum of monomer 2.

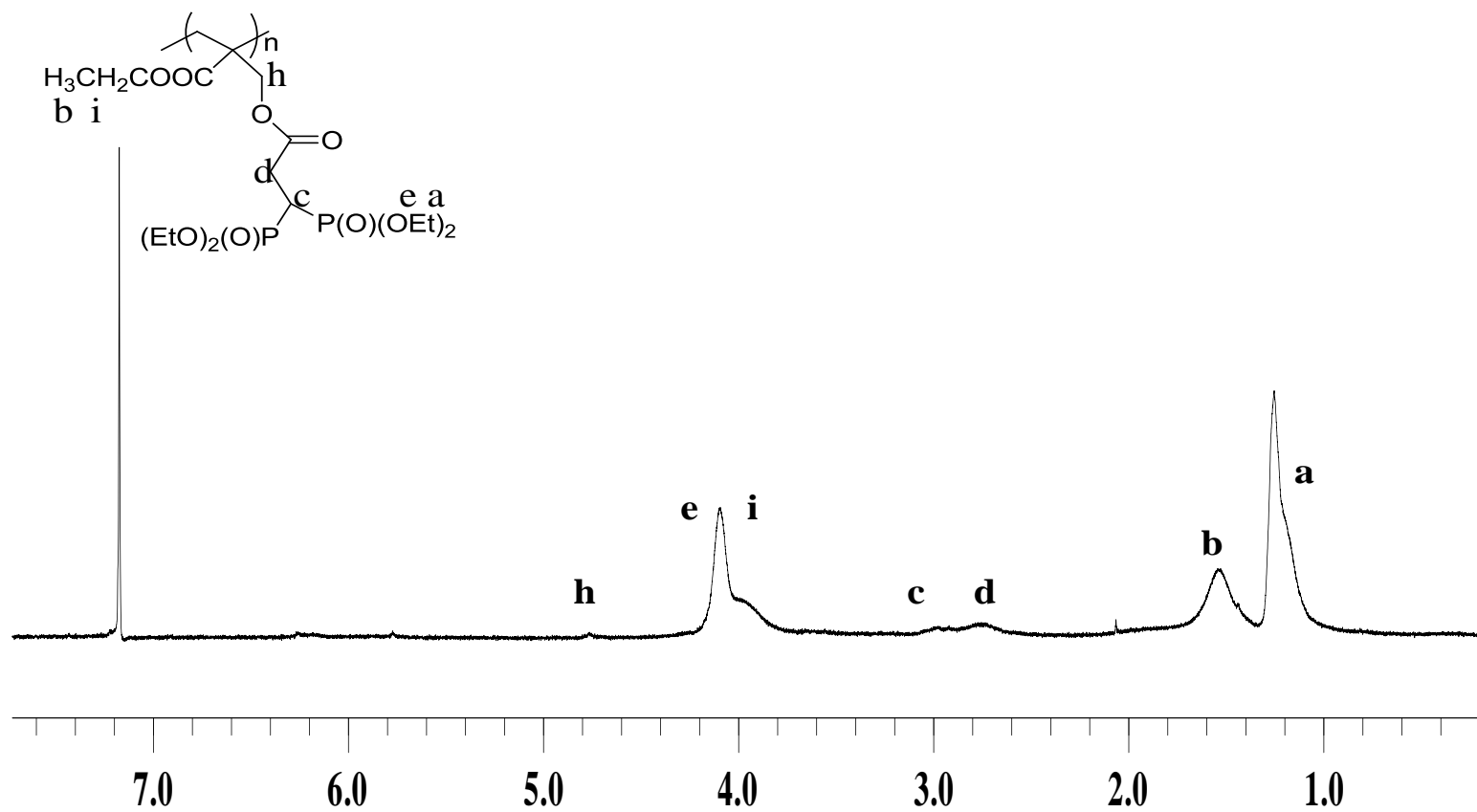


Figure A.7.  $^1\text{H}$  NMR Spectrum of polymer 1 in  $\text{CDCl}_3$ .

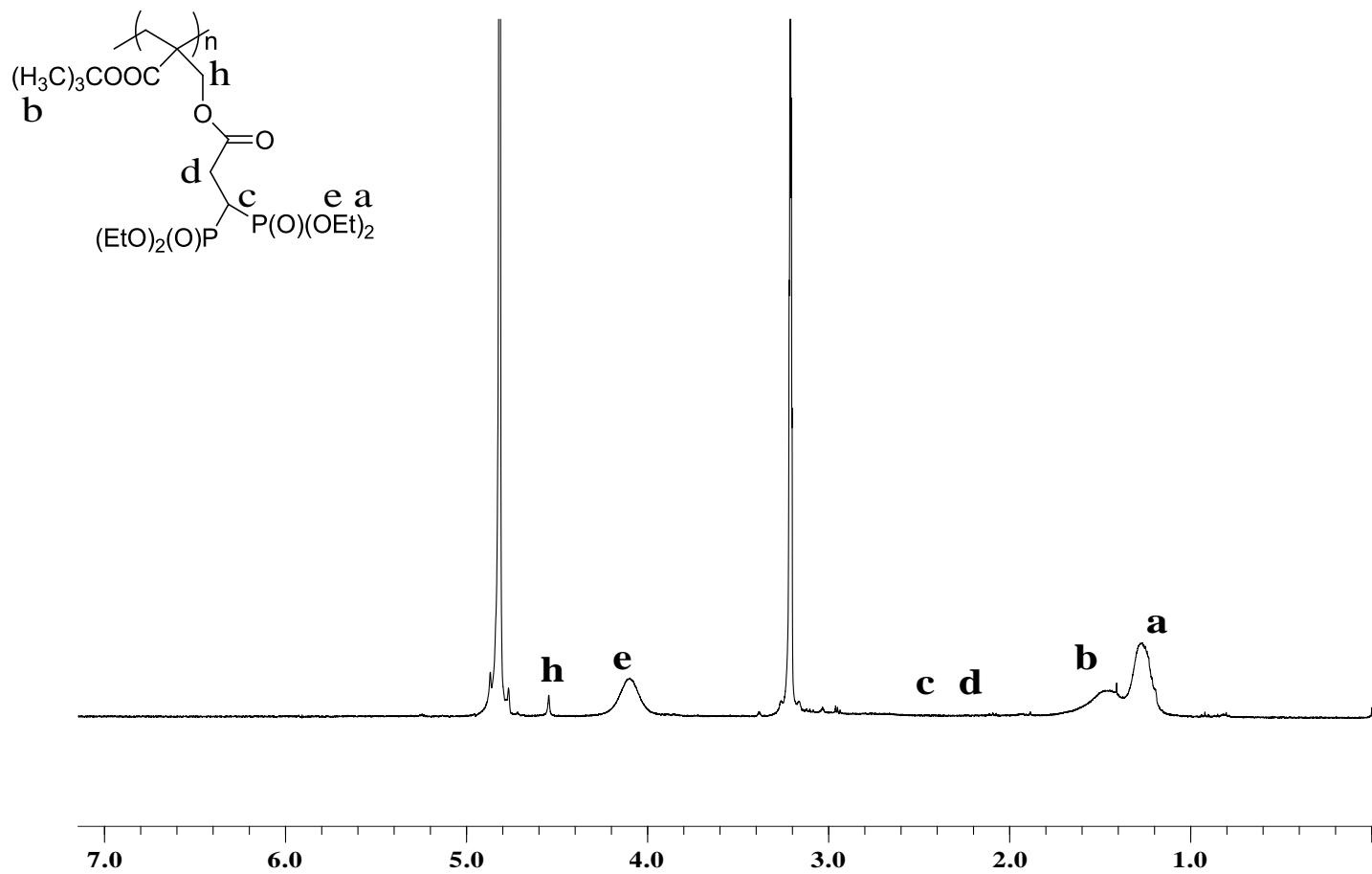


Figure A.8.  $^1\text{H}$  NMR Spectrum of polymer 2 in MeOD.

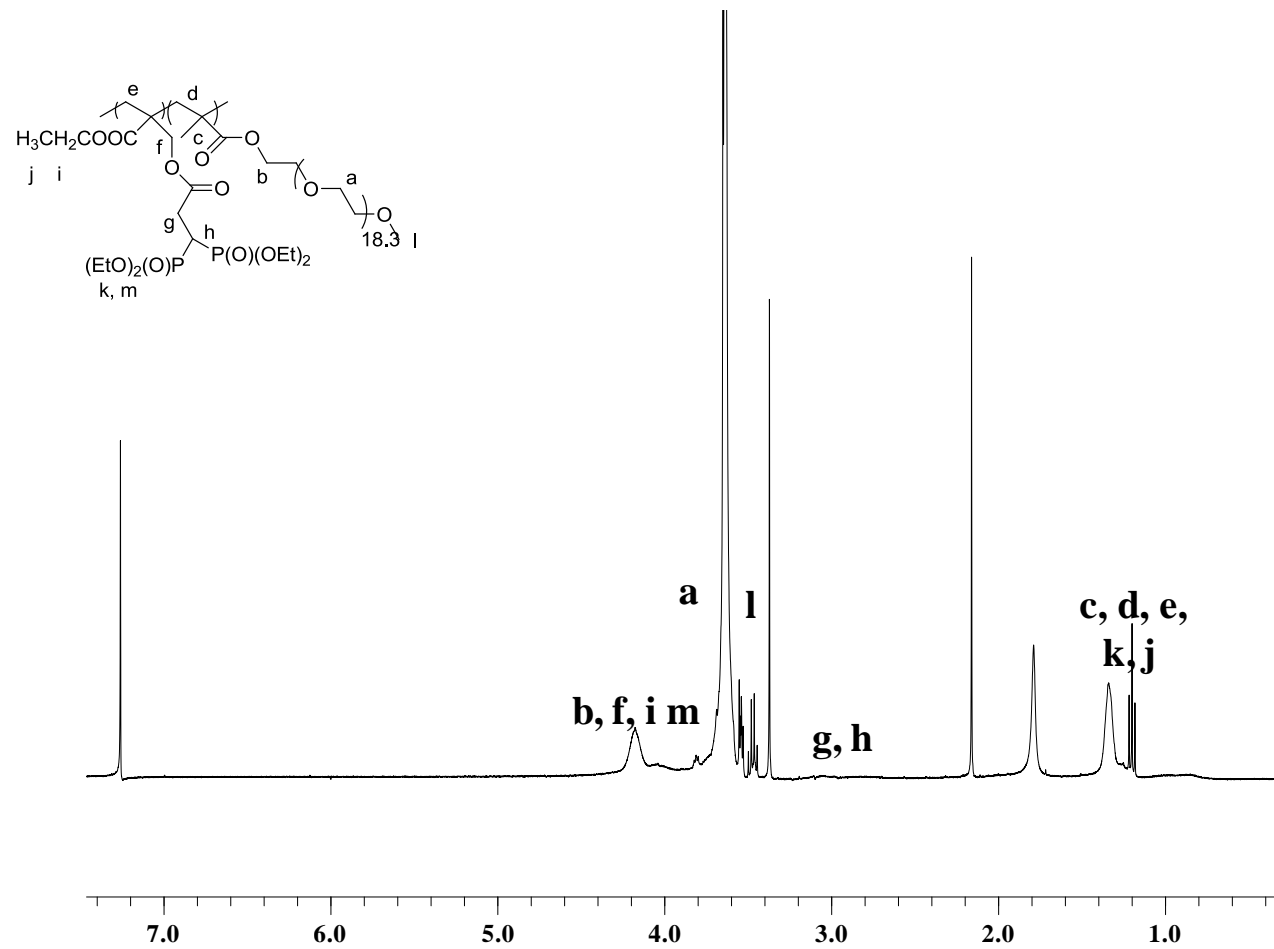


Figure A.9.  $^1\text{H}$  NMR Spectrum of copolymer 1: PEGMA (50:50 mol %) in  $\text{MeOD}$ .

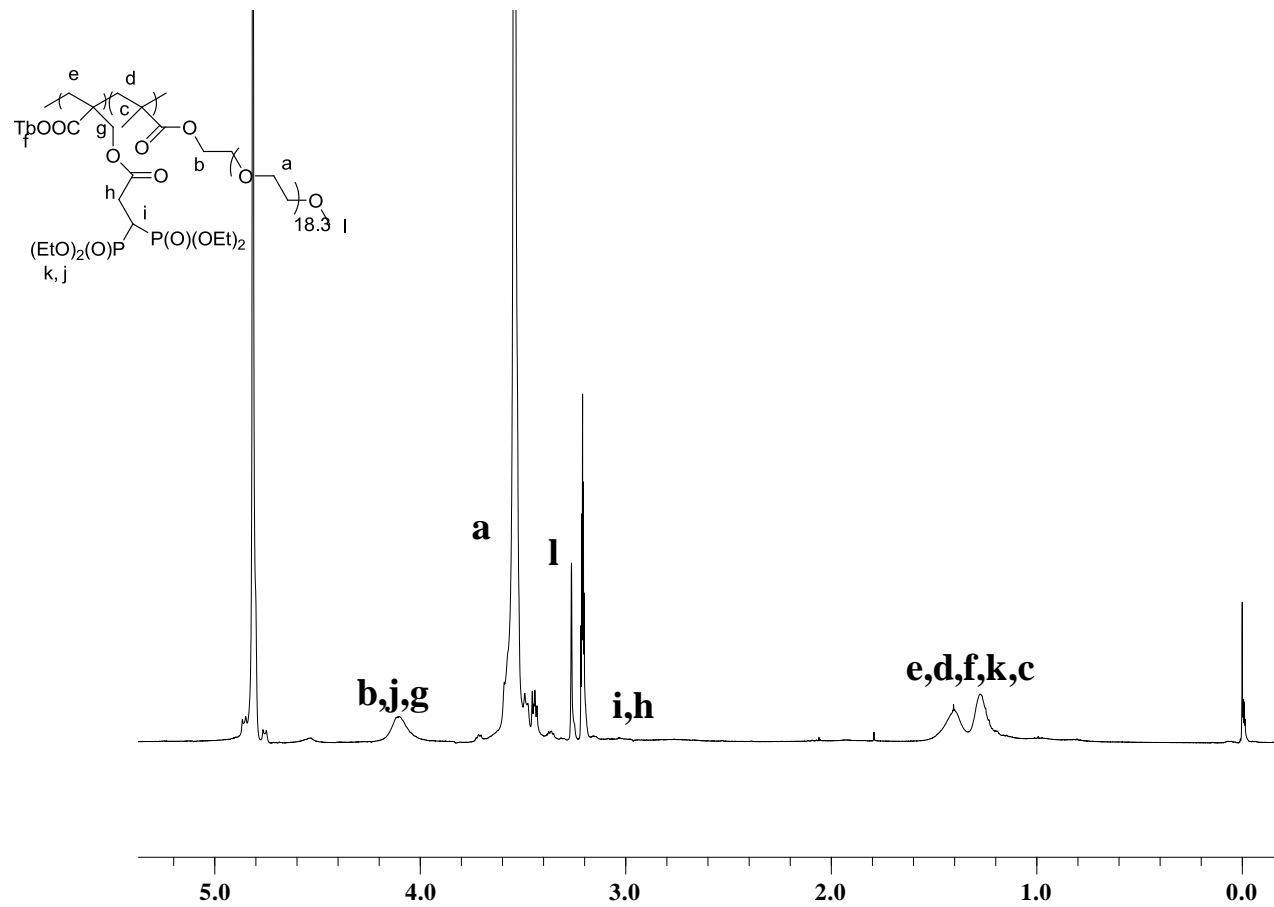


Figure A.10.  $^1\text{H}$  NMR Spectrum of copolymer 2: PEGMA (50:50 mol %) in  $\text{MeOD}$ .

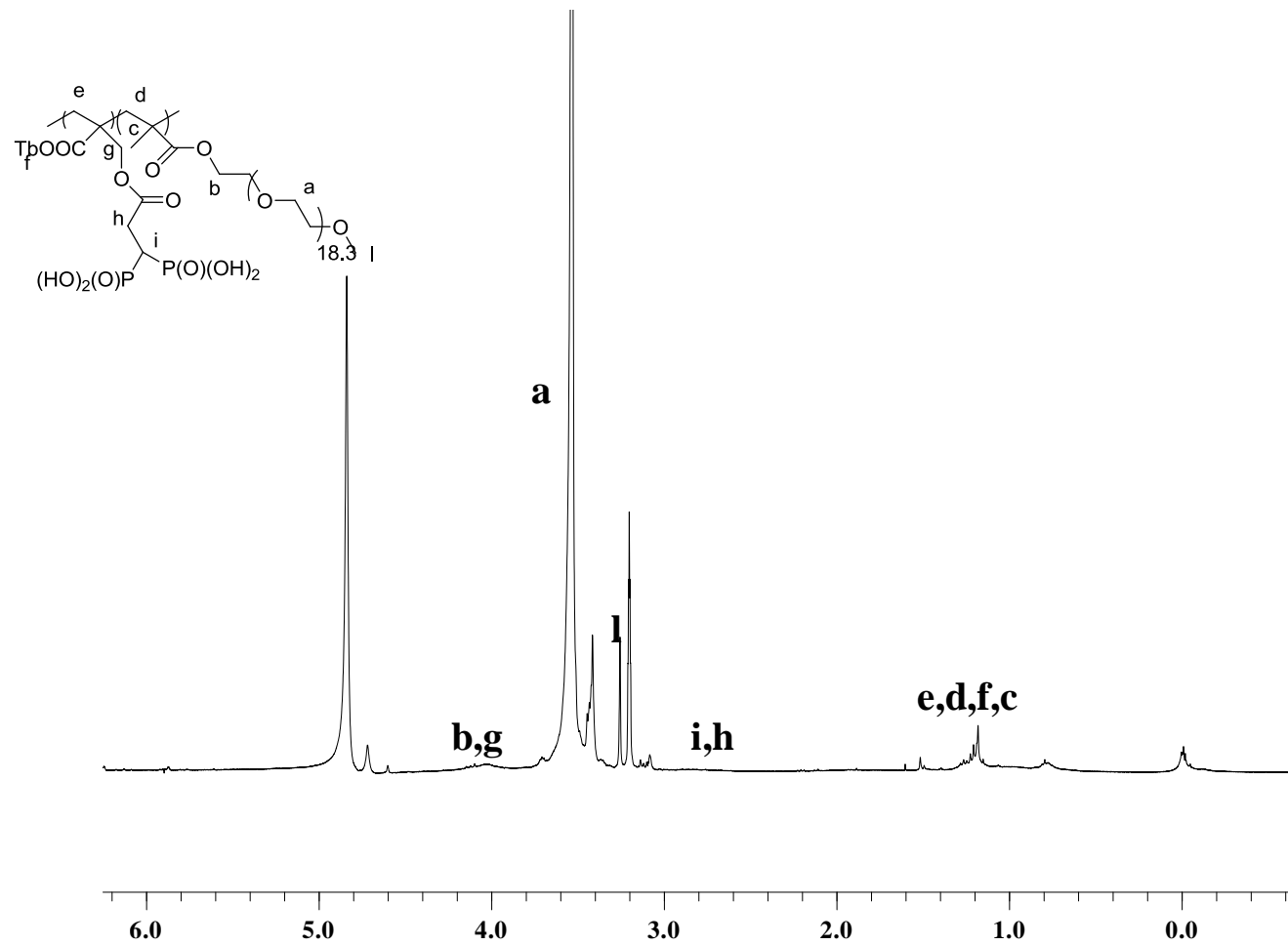


Figure A.11.  $^1\text{H}$  NMR spectrum of hydrolysed copolymer 2: PEGMA (50:50 mol %) in MeOD.

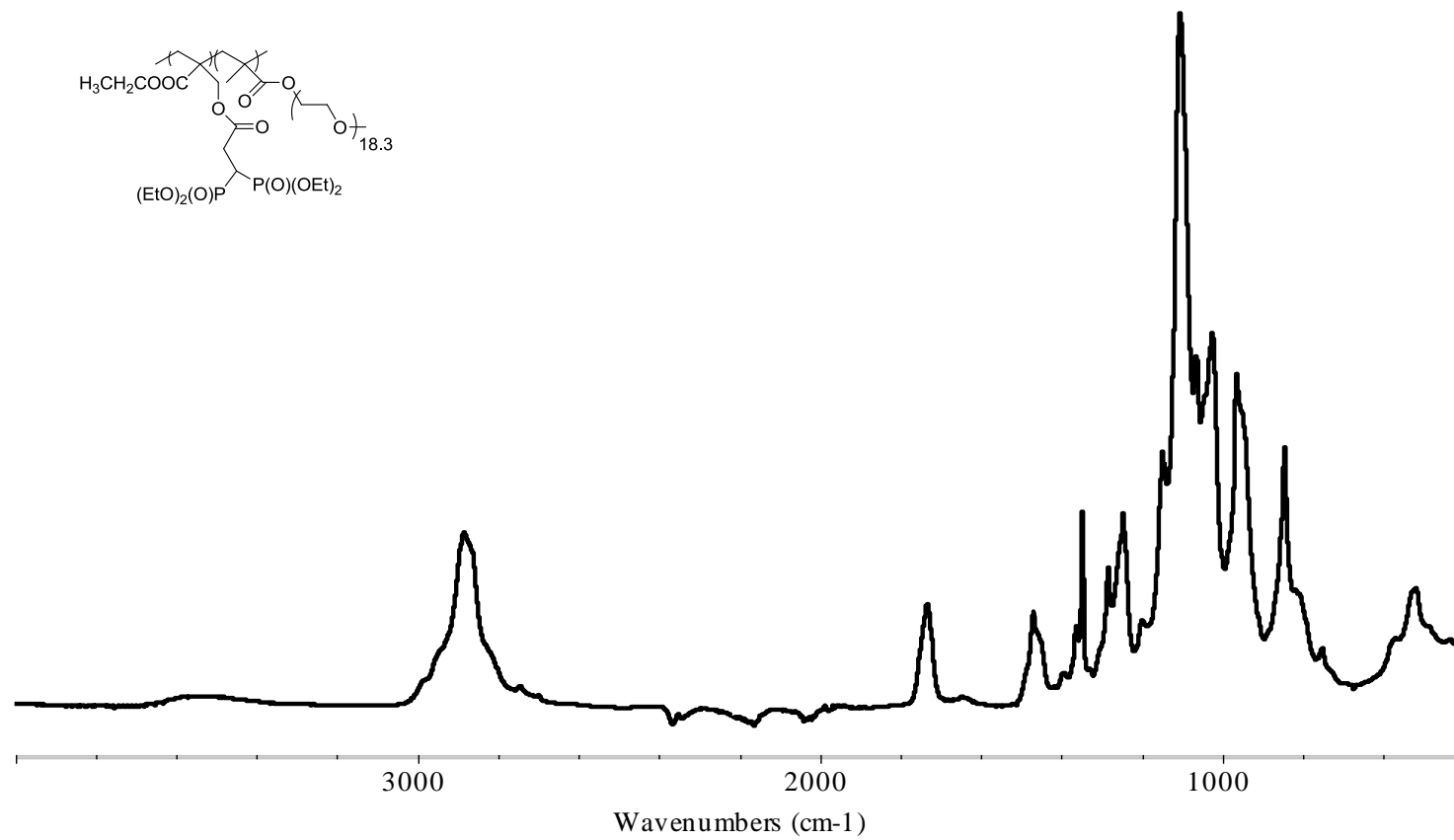


Figure A.12. FTIR spectrum of copolymer 1: PEGMA (50:50 mol %).

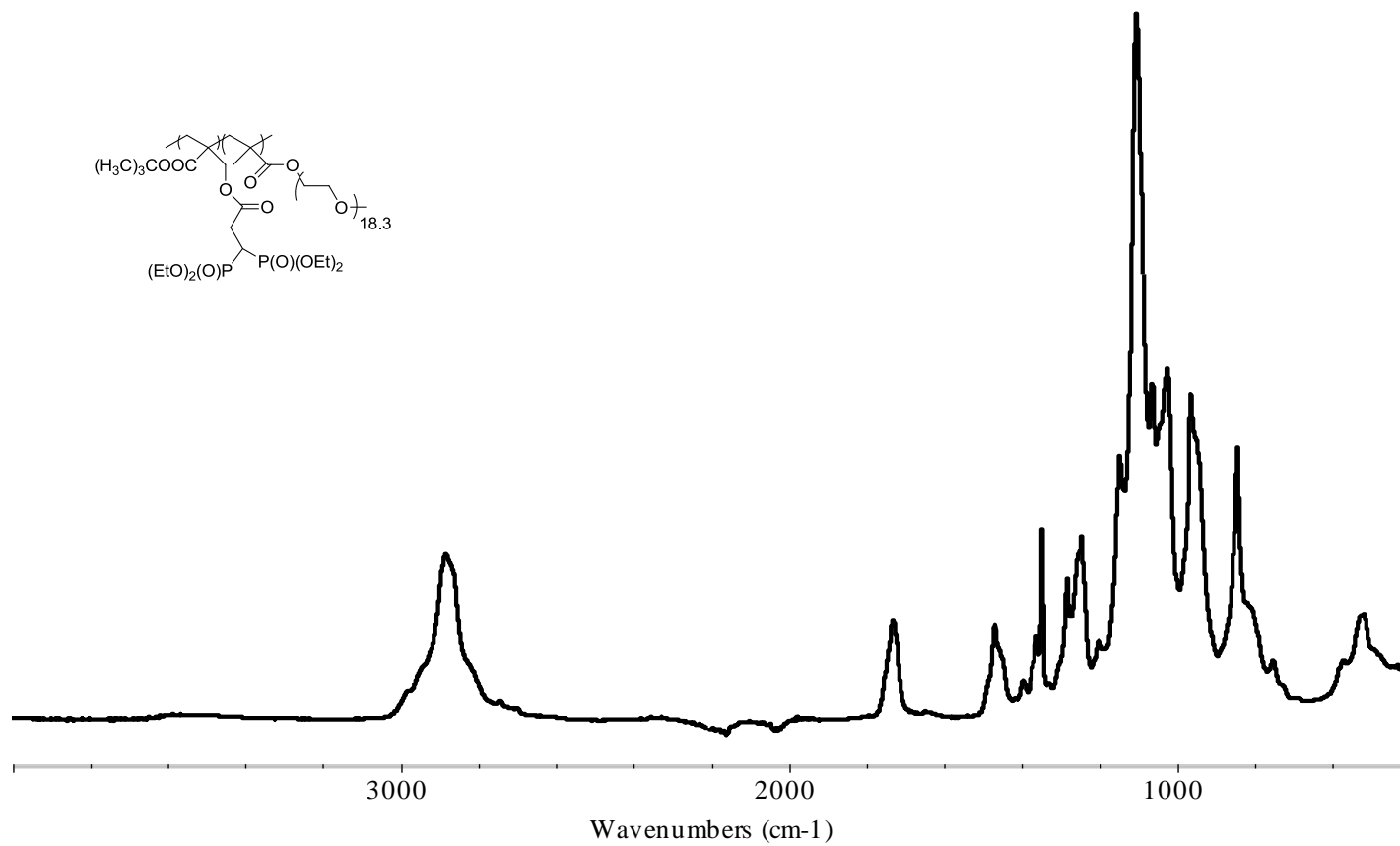


Figure A.13. FTIR spectrum of copolymer 2: PEGMA (50:50 mol %).



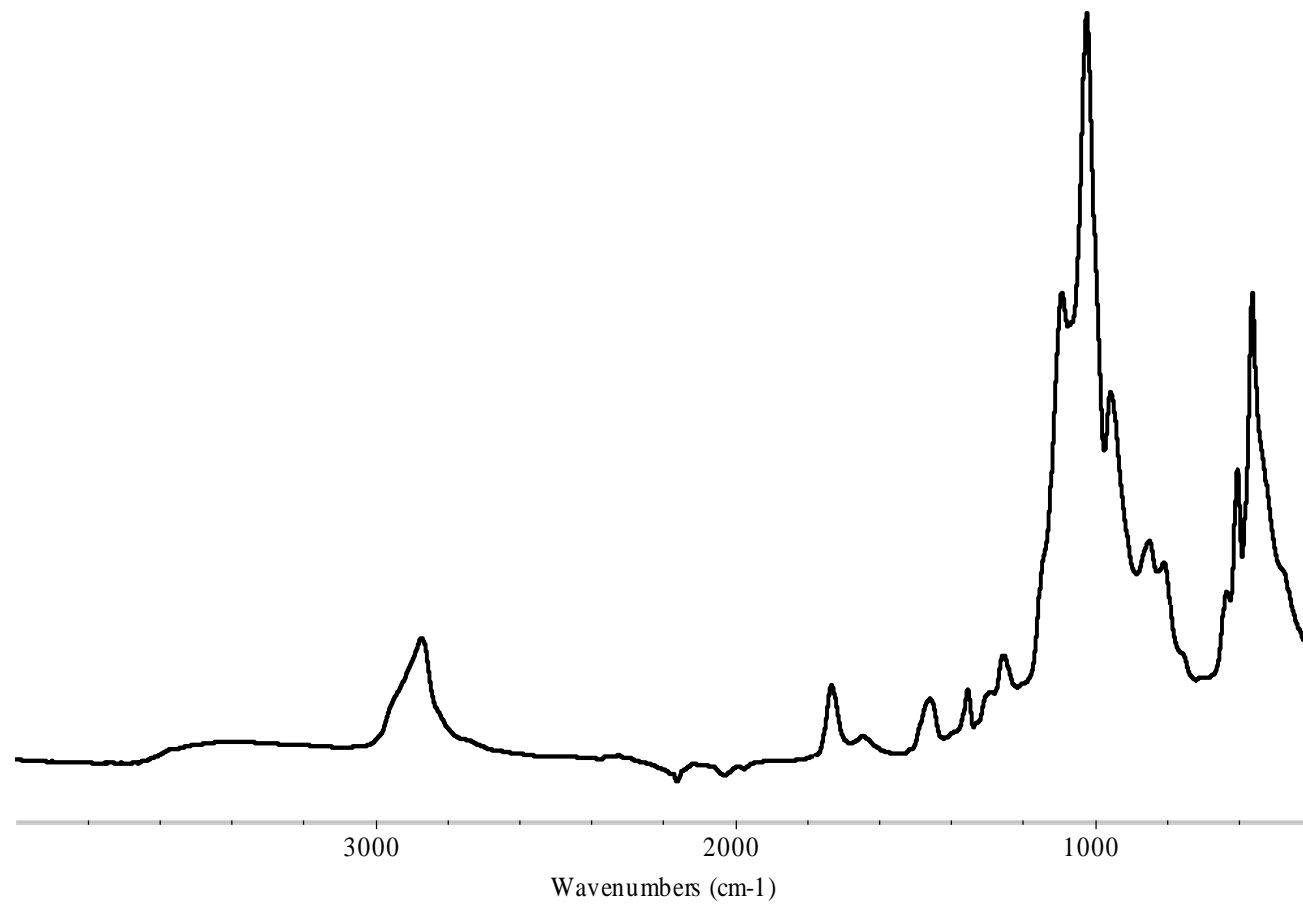


Figure A.15. FTIR spectrum of hydrolysed copolymer 2: PEGMA (50:50 mol %) after addition of 30 mg HAP.

## REFERENCES

1. Zhang, S., G. Gangal and H. Uludag, “Magic Bullets for Bone Diseases: Progress in Rational Design of Bone-seeking Medicinal Agents”, *Chemical Society Reviews*, Vol. 36, pp. 507-531, 2007.
2. Wang, L., *Synthesis and Applications of Bisphosphonate-Based Biomaterials and Nanomaterials* Hong Kong University of Science and Technology, Hong Kong (SAR), P. R. C., 2007.
3. Fleisch, H., “Development of Bisphosphonates”, *Breast Cancer Research*, Vol. 4, pp. 30-34, 2002.
4. Vondracek, S. F., and S. A. Linnebur, “Diagnosis and Management of Osteoporosis in the Older Senior”, *Clinical Interventions Aging*, Vol. 4, pp.121–136, 2009.
5. Rodan, G. A., and T. J. Martin, “Therapeutic Approaches to Bone Diseases”, *Science* Vol.289, pp. 1508-1514, 2000.
6. Lourwood, D.L., “The Pharmacology and Therapeutic Utility of Bisphosphonates”, *Pharmacotherapy*, Vol. 18, pp. 779-789, 1998.
7. Fleisch, H., “Bisphosphonates: Pharmacology and Use in the Treatment of Tumour-Induced Hypercalcaemic and Metastatic Bone Disease”, *Drugs*, Vol. 42, 919-944, 1991.
8. Houghton, T. J., K. S. E. Tanaka, T. Kang, E. Dietrich, Y. Lafontaine, D. Delorme, S. S. Ferreira, F. Viens, F. F. Arhin, I. Sarmiento, D. Lehoux, I. Fadhil, K. Laquerre, J. Liu, V. Ostiguy, H. Poirier, G. Moeck, T. R. Parr and A. R. Far, “Linking Bisphosphonates to the Free Amino Groups in Fluoroquinolones: Preparation of

- Osteotropic Prodrugs for the Prevention of Osteomyelitis”, *Journal of Medicinal Chemistry*, Vol. 51, pp. 6955-6969, 2008.
9. Hirabayashi, H., T. Takahashi, J. Fujisaki, T. Masunaga, S. Sato, J. Hiroi, Y. Tokunaga, S. Kimura and T. Hata, “Bone-specific Delivery and Sustained Release of Diclofenac, a Non-steroidal Anti-inflammatory Drug, via Bisphosphonic Prodrug Based on the Osteotropic Drug Delivery System (ODDS)”, *Journal of Control Release*, Vol. 70, pp. 183-191, 2001.
  10. Gil, L., Y. Han, E. E. Opas, G. A. Rodan, R. Ruel, J. G. Seedor, P. C. Tyler and R. N. Young, “Prostaglandin E<sub>2</sub>-Bisphosphonate Conjugates: Potential Agents for Treatment of osteoporosis”, *Bioorganic and Medicinal Chemistry*, Vol. 7, pp. 901-919, 1999.
  11. Page, P. C. B., M. J. McKenzie and J. A. Gallagher, “Novel Synthesis of Bis(phosphonic acid)-Steroid Conjugates”, *Journal of Organic Chemistry*, Vol. 66, pp. 3704-3708, 2001.
  12. Ogawa, K., T. Mukai, Y. Arano, M. Ono, H. Hanaoka, S. Ishino, K. I. Hashimoto, H. Nishimura and H. Saji, “Development of a Rhenium-186-Labeled MAG3-Conjugated Bisphosphonate for the Palliation of Metastatic Bone Pain Based on the Concept of Bifunctional Radiopharmaceuticals”, *Bioconjugate Chemistry*, Vol. 16, pp. 751-757, 2005.
  13. Kubicek, V., J. Rudovsky, J. Kotek, P. Hermann, L. V. Elst, R. N. Muller, Z. I. Kolar, H. T. Wolterbeek, J. A. Peters and I. Lukes, “A Bisphosphonate Monoamide Analogue of DOTA: A Potential Agent for Bone Targeting”, *Journal of the American Chemical Society*, Vol. 127, pp. 16477-16485, 2005.
  14. Wright, J. E.I., S. A. Gittens, G. Bansal, P. I. Kitov, D. Sindrey, C. Kucharski and H. Uludag, “A Comparison of Mineral Affinity of Bisphosphonate-Protein Conjugates Constructed with Disulfide and Thioether Linkages”, *Biomaterials*, Vol. 27, pp. 769-784, 2006.

15. Bansal, G., J. E. I. Wright, C. Kucharski and H. Uludag, "A Dendritic Tetra(bisphosphonic acid) for Improved Targeting of Proteins to Bone", *Angewandte Chemie International Edition*, Vol. 44, pp. 3710-3714, 2005.
16. Fleisch, H., "Bisphosphonates in Bone disease: From the Laboratory to Patient", *Parthenon Publishing Group*, Vol.3, pp.32-57, 1997.
17. Rodan, G. A., and H. A. Fleisch, "Bisphosphonates: Mechanism of Action", *Journal of Clinical Investigation*, Vol. 97, pp. 2692–2696, 1996.
18. Zhang, S., G. Gangal and H. Uludag, "Magic Bullets' for Bone Diseases: Progress in Rational Design of Bone-seeking Medicinal Agents", *Chemical Society Review*, Vol. 36, pp. 507-531, 2007.
19. Hirabayashi, H., and J. Fujisaki, "Bone-specific Drug Delivery Systems: Approaches Via Chemical Modification of Bone-seeking Agents", *Clinical Pharmacokinetics*, Vol.42, pp. 1319-1330, 2003.
20. Erez R., S. Ebner, B. Attalib, and D. Shabata, "Chemotherapeutic Bone-targeted Bisphosphonate Prodrugs with Hydrolytic Mode of Activation", *Bioorganic & Medicinal Chemistry Letters*, Vol. 18, pp.816-820, 2008.
21. Ehrick R. S., M. Capaccio, D. A. Puleo and L. G. Bachas, "Ligand-Modified Aminobisphosphonate for Linking Proteins to Hydroxyapatite and Bone Surface", *Bioconjugate Chemistry*, Vol. 19, pp. 315–321, 2008.
22. Wang, D., S. Miller, M. Sima, P. Kopeckova and J. Kopecek, "Bone-targeting Macromolecular Therapeutics ", *Advanced Drug Delivery Reviews*, Vol. 57, pp. 1049-1076, 2005.
23. Wang, D., S. C. Miller, P. Kopeckova and J. Kopecek, "Synthesis and Evaluation of Water-Soluble Polymeric Bone-Targeted Drug Delivery Systems", *Bioconjugate Chemistry*, Vol. 14, pp. 853-859, 2003.

24. Miller, K., R. Erez, E. Segal, D. Shabat, and R. S. Fainaro, "Targeting Bone Metastases with a Bispecific Anticancer and Antiangiogenic Polymer–Alendronate–Taxane Conjugate", *Angewandte Chemie International Edition*, Vol.48, pp. 2949–2954, 2009.
25. Miller, K., A. E. Boock, D. Polyak, E. Segal, L. Benayoun, Y. Shaked and R. S. Fainaro, "Antiangiogenic Antitumor Activity of HPMA Copolymer–Paclitaxel–Alendronate Conjugate on Breast Cancer Bone Metastasis Mouse Model", *Molecular Pharmaceutics*, Vol. 8, pp. 1052–1062, 2011.
26. Bhargava, P., J. L. Marshall, N. Rizvi, W. Dahut, J. Yoe, M. Figuera, K. Phipps, V. S. Ong, A. Kato and M.J. Hawkins, "A Phase I and Pharmacokinetic Study of TNP-470 Administered Weekly to Patients with Advanced Cancer", *Clinical Cancer Research* Vol. 5 pp. 1989–1995, 1999.
27. Segal, E., H. Pan, P. Ofek, T. Udagawa, P. Kopeckova, J. Kopecek, and R. S. Fainaro, "Targeting Angiogenesis-dependent Calcified Neoplasms Using Combined Polymer Therapeutics", *PLoS One*, Vol. 4, pp. 1-15, 2009.
28. Segal, E., H. Pan, L. Benayoun, P. Kopeckova, Y. Shaked, J. Kopecek, and R. S. Fainaro, "Enhanced Anti-tumor Activity and Safety Profile of Targeted Nanoscaled HPMA Copolymer–Alendronate–TNP-470 Conjugate in the treatment of bone malignances", *Biomaterials*, Vol. 32, pp. 4450–4463, 2011.
29. Tengvall, P., B. Skoglund, A. Askendal, and P. Aspenberg, "Surface Immobilized Bisphosphonate Improves Stainless Steel Screw Fixation in Rats", *Biomaterials*, Vol. 25, pp. 2133-2138, 2004.
30. Yoshinari, M., Y. Oda, H. Ueki, and S. Yokose, "Immobilization of Bisphosphonates on Surface Modified Titanium", *Biomaterials*, Vol. 22, pp. 709-715, 2001.

31. Ohgushi, H. and A. I. Caplan, "Stem Cell Technology and Bioceramics: From Cell to Gene Engineering", *Journal of Biomedical Materials Research*, Vol. 48, pp. 913-927, 1999.
32. Song, J., E. Saiz, and C. R. A. Bertozzi, "A New Approach to Mineralization of Biocompatible Hydrogel Scaffolds: An Efficient Process Toward 3-dimensional Bone Like Composites", *Journal of American Chemical Society*, Vol. 125, pp. 1236-1243, 2003.
33. Kretlow, J. D. and A. G. Mikos "Review: Mineralization of Synthetic Polymer Scaffolds for Bone Tissue Engineering", *Tissue Engineering*, Vol. 13, pp. 927-938, 2007.
34. Chirila, T. V. and Zainuddin "Calcification of Synthetic Polymers Functionalized with Negatively Ionizable Groups: A Critical Review", *Reactive and Functional Polymers*, Vol. 67, pp. 165-172, 2007.
35. Filmon, R., F. Grizon, M. F. Basle and D. Chappard, "Effects of Negatively Charged Groups (Carboxymethyl) on the Calcification of Poly(2-hydroxyethyl methacrylate)", *Biomaterials*, Vol. 23, pp. 3053-3059, 2002.
36. Wang, L., M. Zhang, Z. Yang and B. Xu, "The first Pamidronate Containing Polymer and Copolymer", *Chemical Communications*, Vol. 26, pp. 2795-2797, 2006.
37. Zhang, S., J. E. I. Wright, N. Özber and H. Uludag, "The Interaction of Cationic Polymers and Their Bisphosphonate Derivatives with Hydroxyapatite", *Macromolecular Bioscience*, Vol. 7, pp. 656-670, 2007.
38. Alferiev, I., N. Vyavahare, C. Song, J. Connolly, J. T. Hinson, Z. Lu, S. Tallapragada, R. Bianco and R. Levy, "Bisphosphonate Derivatized Polyurethanes Resist Calcification", *Biomaterials*, Vol. 22, pp. 2683-2693, 2001.

39. Moszner, N. and U. Salz, "Recent Developments of New Components for Dental Adhesives and Composites", *Macromolecular Materials and Engineering*, Vol. 292, pp. 245-271, 2007.
40. Abuelyaman, A. S., G.S. Boardman, B. A. Shukla, S. M. Aasen, S. B. Mitra, M. Mikulla and D. K. Cinader, "Compositions Including Polymerizable Bisphosphonic Acids and Methods", *US Patent*, US2004206932, 2004.
41. Senaratne, S. G. and K. W. Colston, "The Role of Bisphosphonates in Breast Cancer: Direct Effects of Bisphosphonates on Breast Cancer Cells", *Breast Cancer Research*, Vol.4, pp. 18-23, 2002.
42. Catel, Y., V. Besse, A. Zulauf, D. Marchat, E. Pfund, T. N. Pham, D. Bernache-Assolant, M. Degrange, T. Lequeux, P-J. Madec and L. L. Pluart, "Synthesis and Evaluation of New Phosphonic, Bisphosphonic and Difluoromethylphosphonic Acid Monomers for Dental Application", *European Polymer Journal*, Vol. 48, pp. 318-330, 2012.
43. Lynn J., F. Bala, B. A. Kashemirov and C. E. McKenna, "Synthesis of a Novel Bisphosphonic Acid Alkene Monomer", *Synthetic Communications*, Vol. 40, pp. 3577-3584, 2010.
44. Mathias, L. J., S. H. Kusefoglou, A. O. Kress, S. Lee, C. W. Dickerson and S. F. Thames, "New Acrylate-Containing Dimers and Oligomers for Crosslinking Vinyl Polymers", *Polymer News*, Vol. 17, pp. 36-42, 1992.
45. Mathias, L. J., and S. H. Kusefoglou, "New Difunctional Methacrylate Ethers and Acetals: Readily Available Derivatives of  $\alpha$ -Hydroxymethyl Acrylates", *Macromolecules*, Vol. 20, pp.2039-2041, 1987.
46. Mathias, L. J, R. M. Warren and S. Huang, "Tert-butyl  $\alpha$  -(Hydroxymethyl) Acrylate and Its Ether Dimer: Multifunctional Monomers Giving Polymers with Easily Cleaved Ester Groups", *Macromolecules*, Vol. 24, pp. 2036-2042, 1991.

47. Anseth, K. S., C. M. Wang, C. N. Bowman, "Kinetic Evidence of Reaction-Diffusion during the Polymerization of Multi (Meth) Acrylate Monomers", *Macromolecules*, Vol. 27, pp. 650-655, 1994.
48. Brandrup, J. and E. H. Immergut, "Polymer Handbook", *Wiley-Interscience, New York*, 1975.
49. Karahan, O., D. Avcı and V. Aviyente, "Structure–reactivity Relationships of Alkyl  $\alpha$ -Hydroxymethacrylate Derivatives", *Journal of Polymer Science Part A: Polymer Chemistry*, Vol.49, pp.3058-3068, 2011.